Collaborative platooning and routing for mixed fleets of electric automated vehicles and conventional trucks

Pourmohammad-Zia, Nadia; Negenborn, Rudy R.; Schulte, Frederik

DOI
10.1111/itor.70073

Publication date
2025

Document Version
Final published version

Published in
International Transactions in Operational Research

Citation (APA)
Pourmohammad-Zia, N., Negenborn, R. R., & Schulte, F. (2025). Collaborative platooning and routing for mixed fleets of electric automated vehicles and conventional trucks. *International Transactions in Operational Research*. https://doi.org/10.1111/itor.70073

INTERNATIONAL TRANSACTIONS IN OPERATIONAL RESEARCH

WILEY

INTERNATIONAL TRANSACTIONS IN OPERATIONAL RESEARCH

Intl. Trans. in Op. Res. 0 (2025) 1–41
DOI: 10.1111/itor.70073

Collaborative platooning and routing for mixed fleets of electric automated vehicles and conventional trucks

Nadia Pourmohammad-Zia[a,*], Rudy R. Negenborn[b] and Frederik Schulte[b]

[a] *Department of Hydraulic Engineering, Delft University of Technology, 2628 CN Delft, The Netherlands*
[b] *Department of Maritime and Transport Technology, Delft University of Technology, 2628 CD Delft, The Netherlands*
E-mail: n.pourmohammadzia@tudelft.nl [Pourmohammad-Zia]; r.r.negenborn@tudelft.nl [Negenborn]; F.Schulte@tudelft.nl [Schulte]

Received 14 October 2024; received in revised form 7 May 2025; accepted 27 June 2025

Abstract

The application of automated ground vehicles (AGVs) is well-established in closed environments such as port terminals, while their operation in open areas remains challenging. In this work, we set out to overcome this limitation by introducing platooning as a transfer mode in heterogeneous vehicle networks. We propose a collaborative transportation framework where different transportation companies use a shared platform for delivery tasks. To support decarbonization efforts in port hinterland transport, we consider fleets comprising electric AGVs (E-AGVs) and conventional trucks. These E-AGVs need to visit charging stations, modeled as battery swap stations (BSS), and join platoons to travel within the linking road segment. Each carrier has contracts with certain BSSs and shares these stations through the platform as part of the transportation plan. The platform functions as a demand and resource pooling mechanism, further offering platooning and infrastructure-sharing services. We model the interaction between the platform and carriers as a two-level constrained Stackelberg competition. An efficient solution algorithm, incorporating problem-specific heuristics and an adaptive large neighborhood search with dedicated destroy, repair, and intensification operators, is proposed. Extensive numerical experiments demonstrate the algorithm's performance on both existing and new benchmark instances. Our results highlight the platform's potential to streamline port-hinterland logistics, with E-AGV platoons significantly reducing costs and emissions.

1. Introduction

The logistics and freight transportation sectors are evolving rapidly due to advanced technologies and innovative business models, with autonomous vehicle technology being particularly transformative. Autonomous ground vehicles (AGVs) offer increased efficiency, reduced labor costs, environmental sustainability, and enhanced safety. Initially used in controlled environments like

*Corresponding author.

ports and industrial complexes, AGVs are now poised for integration into broader transportation networks.

However, the rapid advancements in AGV technology have not been matched by corresponding improvements in physical infrastructure, confining AGVs to closed environments and limiting their applicability (Caballero et al., 2023). Platooning, where vehicles travel closely together, led by a human-driven vehicle and coordinated by advanced communication systems, addresses this challenge. It enhances road utilization, bridging the gap between closed environments and broader networks. With a human driver leading, platooning improves safety, and efficiency, and reduces fuel consumption and emissions through aerodynamic efficiency and synchronized driving (Pourmohammad-Zia et al., 2020; Bhoopalam et al., 2018).

The evolution towards autonomous transportation is complemented by the rise of platforms. While ride-sharing and mobility platforms have demonstrated the transformative power of digital ecosystems in transportation, the logistics industry has yet to fully embrace these platforms. Given the high capital investment and limited availability of AGVs, their underutilization is greatly undesirable. Logistics platforms can connect carriers with shippers and receivers, facilitating efficient resource allocation and reducing empty runs. These platforms not only enable demand and resource pooling but also can facilitate battery pooling. This is crucial for AGVs, as they predominantly rely on electricity and have a shorter driving range compared to normal trucks. Through the synergies among AGVs, platooning strategies, and platform-based collaboration, the logistics industry can achieve new levels of efficiency, cost-effectiveness, and sustainability. In particular, platforms are envisioned not only as digital brokers but as centralized coordination agents that optimize the use of shared resources across multiple carriers. This reflects a growing trend in collaborative logistics, where platforms take an active role in managing demand and resource pooling, including routing, platooning, and infrastructure access. These services are contractually delegated by participating carriers, and platform-generated plans are subject to their acceptance, preserving operational autonomy. This vision is increasingly reflected in real-world practices. Shared warehouse and container-reuse platforms already enable neutral coordinators to manage shared assets across independent stakeholders. A notable example is Koopman Logistics Group in Europe, which has piloted collaborative vehicle routing and platooning with centrally coordinated, cross-carrier route matching. These examples illustrate that the structure we propose is not only conceptually sound but also aligned with emerging logistics models.

Inspired by the aforementioned advantages, this paper explores the potential of integrating autonomous technology with logistics platforms, where different carriers join a platform to execute delivery tasks. The transportation network is heterogeneous, featuring vehicle depots and demand points in areas with suitable road and communication infrastructure for autonomous driving, while the linking road segments between these areas remain unsuitable for AGVs. Carriers operate fleets that include electric AGVs (E-AGVs) with limited travel ranges and conventional trucks. Despite the potential of E-AGVs to improve transportation systems by reducing driver dependency and emissions, their application faces two significant challenges: the need for frequent charging and the necessity to join a platoon for travel on non-AGV-ready road segments. Charging stations, designed as battery swap stations (BSS), facilitate quick battery replacements, thereby eliminating prolonged vehicle downtime. Each carrier has contracts with specific BSSs and shares access to these stations with the platform as part of the transportation plan. The platform's battery pooling service effectively addresses the issue of battery ownership inherent in

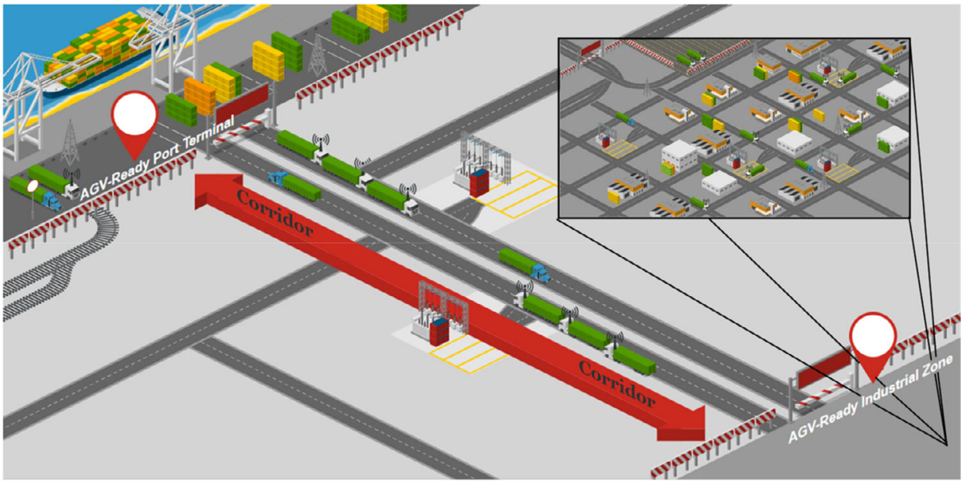

Fig. 1. An application area for AGV platoons.

battery swapping schemes. The platform's problem is modeled as a platooning and mixed fleet routing problem, where it determines transportation routes and service fees for both E-AGVs and conventional trucks. Based on these directives, carriers decide whether to deploy E-AGVs or conventional trucks for different delivery tasks. This interactive decision-making process is modeled as a two-level constrained Stackelberg competition. This framework demonstrates significant potential for enhancing transportation efficiency between logistics hubs via major corridors (see Fig. 1).

The main contributions of the paper, essential for advancing smart transportation logistics, include

- integration of E-AGVs with battery swap options into collaborative vehicle routing and platooning (see Table 1 for comparison with existing literature);
- fusion of Electric Vehicle Routing Problem (EVRP) and corridor electrification to optimize local and long-distance electric vehicle routing, enhancing efficiency and cost-effectiveness in mixed fleets;
- presentation of platooning as a "transfer mode," extending AGVs application beyond closed environments, thus contributing to improved logistics performance;
- provision of a platform facilitating demand and resource pooling among carriers and demand points, along with crucial services, including platooning coordination and battery pooling, effectively mitigating the challenges of limited and costly availability of E-AGVs, the complexity of platoon formation, and the issue of battery ownership, respectively.
- modeling of the interactive decision-making between the platform and carriers as a two-level Stackelberg competition, enabling carriers to make informed decisions based on their unique cost structures and fostering robust, sustainable relationships within the platform;
- development of an efficient solution algorithm incorporating problem-specific heuristics, adaptive large neighborhood search (ALNS) with local search, and a BSS positioning optimization (BPO) algorithm for intensification, which improves existing benchmark solutions and performs effectively on newly generated instances.

Table 1
General overview of the existing literature

Reference	Features						Scope			
	Platforms	Infrastructure sharing	Electric vehicles	Platooning	AGVs	Heterogeneous vehicle network	Pricing	Routing	Modeling	Solution approach
Yan et al. (2020)	√						√		NLP	Analytic solution
Al-Kanj et al. (2020)	√				√		√		MILP	Approximate DP
Sun et al. (2019)	√						√		NLP	Analytic solution
Lin et al. (2021)	√						√		NLP	Analytic solution
Kung and Zhong (2017)	√						√		NLP	Analytic solution
Hu & Zhou (2020)	√						√		NLP	Analytic solution
Li et al. (2020)	√						√		MILP	Heuristic
Atasoy et al. (2020)	√						√		MILP	Commercial solver
Wang and Huang (2021)	√						√		NLP	Analytic solution
Zhang et al. (2017a)	√							√	MILP	Heuristic
Zhang et al. (2019)	√							√	MILP	Commercial solver
Behrend et al. (2019)	√	√						√	MILP	Branch and price
Ma et al. (2020)	√	√							MILP	Heuristic
Larsson et al. (2015)				√				√	MILP	Heuristic
Sokolov et al. (2017)				√				√	MILP	Heuristic
Zhong et al. (2017)				√					MO MILP	Genetic algorithm
Zhang et al. (2017b)				√				√	NLP	Analytic solution

Continued

Table 1
(Continued)

Reference	Features						Scope			
	Platforms	Infrastructure sharing	Electric vehicles	Platooning	AGVs	Heterogeneous vehicle network	Pricing	Routing	Modeling	Solution approach
Nourmohammad and Hartman (2016)				√				√	MILP	Genetic algorithm
Calvo and Mathar (2018)				√					GT	Analytic solution
Boysen et al. (2018)				√	√				MILP	Heuristic
Scherr et al. (2019)				√	√	√		√	MILP	Commercial solver
You et al. (2020)				√	√			√	MILP	Ant colony
Xue et al. (2021)				√	√			√	MILP	Tabu search
Caballero et al. (2022)				√	√			√	MILP	Heuristic
Luo and Larson (2022)				√				√	MILP	Heuristic
Scholl et al. (2023)			√	√					MILP	ALNS
Johansson et al. (2021)				√					GT	Analytic solution
Pourmohammad-Zia et al. (2023)				√	√	√			MILP	Commercial solver
This work	√	√	√	√	√	√	√	√	MILP/GT	Heuristics + ALNS

Abbreviations: AGVs, automated ground vehicles; ALNS, adaptive large neighborhood search; DP, dynamic programming; GT, game theory; MILP, mixed integer linear programming; MO, multiobjective; NLP, nonlinear programming.

2. Literature review

This research mainly builds on two streams of literature: platform-based collaborative transportation and platooning, each of which will be briefly reviewed. The mixed-fleet routing of E-AGVs and conventional trucks also aligns with the multimodal routing problem stream. For further insights into recent developments, interested readers are referred to Afrasyabi et al. (2023), Kashmiri and Lo (2024), and Farahmand-Tabar and Afrasyabi (2024).

2.1. Platform-based collaborative transportation

The sharing economy significantly enhances efficiency in complex transportation networks (Tang et al., 2023). Collaborative transportation platforms, gaining attention from practitioners and researchers, are emerging as new business models. Despite a decade of research, most studies emphasize theoretical models, applications, and empirical studies, overlooking tactical and operational decisions. Our review highlights recent developments and the potential role of operations research. For further studies, see Alnaggar et al. (2021).

Pricing plays a crucial role in incentivizing participation in platform-based transportation problems, as seen in studies on taxi hailing (Yan et al., 2020; Al-Kanj et al., 2020), ride sharing (Sun et al., 2019; Lin et al., 2021), and freight delivery (Kung and Zhong, 2017; Hu and Zhou, 2020; Li et al., 2020). Atasoy et al. (2020) used dynamic pricing as an incentive for carriers in a platform-based pickup and delivery system to optimize platform costs. Their findings demonstrated that such incentives could increase carriers' profit margins while enhancing the platform's profitability. Wang and Huang (2021) analyzed platform participation from the perspective of competing logistics firms. Their results generally favored platform cooperation for achieving higher profits.

There is a strong demand for efficient logistics systems in B2B e-commerce, where transportation platforms can take a leading part. Zhang et al. (2017a) investigated an e-commerce logistics platform where different logistics service providers share their transportation tasks and vehicles to enhance their profit and vehicle utilization. They showed that higher cooperation brings more benefits to the carriers. Zhang et al. (2019) proposed a relatively similar model for minimizing the total cost of the involved parties. In contrast to all these studies, our study goes beyond pricing and demand–resource pooling to include advanced platform services like platooning and infrastructure sharing. These additions enhance operational efficiency for mixed fleets and tackle routing and resource allocation complexities.

The concept of platform-enabled infrastructure-sharing, widely successful in energy and telecommunications, is still emerging in transportation literature. Behrend et al. (2019) explored item-sharing among crowd shippers, pooling intermediate locations to enhance platform profitability. Ma et al. (2020) addressed regional refueling stations in a taxi-hailing platform, also showing increased profitability through shared facilities. While these studies focus on infrastructure sharing in simplified models, they overlook the dynamic interactions enabled by game theory principles. In contrast, our study integrates platooning services into demand and resource pooling, alongside infrastructure sharing, addressing electric vehicles, autonomy, and complex stakeholder interactions through a game-theoretic framework.

2.2. Platooning

With the rapid advancement of wireless communications, platooning has emerged as a vital strategy for improving road safety, increasing road capacity, and reducing fuel consumption (Pourmohammad-Zia et al., 2020). However, much of the existing literature on platooning focuses heavily on technical aspects such as string stability, longitudinal control, speed profiles, obstacle avoidance, and intraplatoon communications (Bhoopalam et al., 2018).

The literature on platooning in logistics networks is still limited. Larsson et al. (2015) developed a model optimizing fuel consumption in transportation networks through truck platooning-routing, demonstrating significant fuel savings in a German case study. Zhong et al. (2017) investigated platoon coordination and scheduling to minimize fuel consumption and schedule miss penalties, finding limitations in networks with converging routes. Zhang et al. (2017b) also addressed freight transport planning with platoon coordination under travel time uncertainty, showing that platooning is less beneficial on converging routes and when arrival times vary significantly. Nourmohammadzadeh and Hartmann (2016) explored a similar problem, allowing admissible detours for platoon formation. Boysen et al. (2018) analyzed the platoon formation process along a single path, highlighting how factors such as platooning diffusion, maximum platoon length, and time window tightness can significantly influence efficiency. Scholl et al. (2023) focused on electric truck platooning for long-haul transportation, coordinating charging times with platoon wait periods along predetermined routes. These studies primarily focus on fuel savings through platooning for conventional trucks and do not incorporate the integration of autonomy and heterogeneous vehicle networks into platooning and routing, which constitutes a primary focus of our work.

Platooning, depicted effectively through game theory, involves interactive decision-making among vehicles in a convoy. Calvo and Mathar (2018) utilized cooperative game theory to identify a coalition of vehicles within a platoon that minimizes fuel consumption and congestion taxes. Sokolov et al. (2017) presented a coordinated approach to routing and departure time scheduling for platoon-capable vehicles, demonstrating the benefits of centralized coordination over ad hoc platoon formation. Johansson et al. (2021) addressed scenarios where vehicles from different fleet owners operate independently, treating the problem as a noncooperative game. Here, vehicles determine their departure times based on platoon joining decisions to minimize fuel consumption and penalties for delayed departures. Luo and Larson (2022) proposed an iterative route-then-schedule heuristic for centralized platoon planning, showing its computational efficiency through real-world road network experiments. While using the power game theory effectively, these studies overlook the operational aspects, such as routing, lacking integration with comprehensive platform-based coordination, as in our study.

Caballero et al. (2022) investigate truck platooning with a focus on labor cost reduction, analyzing the impact of driver compensation policies and shipment timing flexibility, and proposing heuristics to handle large-scale problems. Scherr et al. (2019) investigated a parcel delivery problem in a heterogeneous infrastructure where autonomous vehicles may drive in AV-ready zones and need to be guided by conventional vehicles in others. They developed a linear programming model for which the problem complexity is reduced by utilizing a time-expanded network that discretizes the planning horizon. You et al. (2020) and Pourmohammad-Zia et al. (2023) studied a similar problem in a full-container setting. Later, Xue et al. (2021) extended this work (You et al., 2020) by developing a Tabu search heuristic to solve the problem. You et al. (2020) and Xue et al. (2021)

do not consider the heterogeneous vehicle network, meaning that AGVs can only move in platoons throughout the network. To the best of our knowledge, these are the only papers in the literature where platooning plays the role of a transfer mode. However, they do not account for collaborative platforms, which are pivotal for managing the limited availability of AGVs. Furthermore, these studies do not integrate electric vehicles, despite the reliance of AGVs on electricity (for a detailed comparison, please refer to Table 1).

Treating platooning as a transfer mode aligns with the concept of connected corridors, critical transportation arteries equipped with advanced vehicle-to-vehicle and vehicle-to-infrastructure communications. These corridors enhance traffic flow, safety, accessibility, and economic growth, attracting global government interest, including the Netherlands (Top Corridors Program, 2018), the United States (Connected Corridors Program, 2014), the United Kingdom (Intercor Project, 2016), and European Commission involving 29 European countries (Cross-border Corridors Project, 2017).

Table 1 provides a general overview of the existing literature on platform-based collaborative transportation and platooning.

In conclusion, the literature review reveals a significant gap in studies focusing on operational and tactical decisions. The existing body of literature is notably sparse, necessitating further investigation into the impact of platforms and platoons on logistics network operations. Current approaches predominantly employ centralized optimization schemes for platform management, overlooking interactive decision-making dynamics among partners and their capabilities, with pricing as a primary point. While existing platforms primarily concentrate on demand and supply pooling, other potential opportunities, such as service and infrastructure-sharing, remain largely unexplored. Despite the potential of electric vehicles to optimize travel costs and emissions, their integration into literature remains limited. Regarding platooning, emphasis is predominantly placed on fuel cost savings, while broader benefits are underexplored. The capacity of platoons to connect diverse zones within heterogeneous networks, termed "platooning as a transfer mode," is crucial for future developments in freight transportation and logistics corridors. Given the complexity arising from integrating platooning with other logistics decisions, sophisticated solution approaches are required for addressing larger-scale instances of this multifaceted problem.

3. Problem description and mathematical model

We address a vehicle routing problem in a heterogeneous network with autonomous and nonautonomous zones. The depot and demand points are in areas accessible to AGVs, but AGVs require platooning on nonautonomous segments. Typical scenarios include freight transport between a port and an industry cluster. Each customer can be served by an E-AGV or a truck. Due to the limited range, E-AGVs need to visit BSSs to replace their batteries.

Vehicles are owned by various carriers, each of which has contracts with specific BSSs and shares access to these stations with the platform as part of the transportation plan. The platform's battery pooling service effectively addresses the issue of battery ownership inherent in battery swapping schemes. Additionally, the platform is responsible for generating a centralized delivery plan, assigning customer demands to available vehicles in a cost-efficient and collaborative manner. This structure, where a neutral coordinating platform proposes assignments that carriers may accept or reject, supports demand and resource pooling, and is increasingly investigated in platform-based logistics.

Vehicles within carriers are homogeneous for each mode but differ across carriers in capacity, acquisition cost, and energy consumption. Despite these differences, all vehicles employ similar batteries, allowing them to share BSS facilities and are compatible for platooning. This compatibility is achieved through standardized V2V communication protocols, interoperable hardware (sensors, actuators, etc), standardized platooning control algorithms, and cybersecurity protocols.

The platform supports collaboration by enabling demand, resource, and battery pooling. It also offers a platooning service for E-AGVs, assigning a driver to lead the platoon and coordinating platooning. These pooling and coordination services require system-wide visibility and trust, which are best facilitated by a neutral platform. While carriers retain full ownership and control of their fleets, the platform's planning function is contractually authorized, ensuring mutual benefit while maintaining carrier autonomy. This hybrid model reflects evolving freight ecosystems where platforms play an active, yet bounded, operational role.

The problem and its outlined assumptions are motivated by emerging developments in freight automation infrastructure. For example, the Dutch Top Corridors Program (Top Corridors Program, 2018) and several EU-supported physical Internet initiatives have identified strategic freight corridors for deploying platooning, electrification, and shared services. Pilots have demonstrated the feasibility of integrating semiautonomous vehicles with standardized V2V communication protocols and corridor-based platooning schemes. Similarly, BSS is being piloted in densely trafficked freight corridors to support commercial EVs. While full interoperability and system-wide infrastructure are not yet widespread, our framework aligns with expected near-future capabilities, particularly in structured, corridor-based logistics networks.

The problem is modeled on a directed graph G(V, E). $V = \{ID\} \cup CSO_1 \cup \{PZ_1\} \cup \vartheta_D \cup CI' \cup \{PZ_2\} \cup CSO_2 \cup \{FD\}$ includes the initial depot (ID) and its copy as the final depot (FD), the set of charging stations in the linking segment between two zones (CSO_1) and its copy to project the stations on the way back (CSO_2), a node in the target zone where E-AGVs disjoin the platoon (PZ_1), and its copy (PZ_2), the set of demand points (ϑ_D), and the set of dummy nodes illustrating the charging stations (CI) within the target zone multiple times (CI'). These copies allow for multiple visits to the stations. The admissible arcs are defined based on vehicle modes (n). $E = \{(i, j)|\ i, j \in V, i \neq j, (i, j) \in A \cup B\}$, where A and B are the sets of admissible arcs for $n = 1$ (E-AGVs) and $n = 2$ (trucks), respectively. $A = A_1 \cup A_2 \cup A_3 \cup A_4 \cup A_5 \cup A_6 \cup A_7$ and $B = B_1 \cup B_2$:

$$A_1 = \{ (i, j) \mid i = ID, j \in CSO_1 \cup \{PZ_1\}\}, \qquad A_2 = \{ (i, j) \mid i \in CSO_1, j \in CSO_1 \cup \{PZ_1\}\},$$

$$A_3 = \{ (i, j) \mid i = PZ_1, j \in \vartheta_D \cup CI'\}, \qquad A_4 = \{ (i, j) \mid i \in \vartheta_D, j \in \vartheta_D \cup CI' \cup \{PZ_2\}\},$$

$$A_5 = \{ (i, j) \mid i \in CI', j \in \vartheta_D \cup CI' \cup \{PZ_2\}\}, \qquad A_6 = \{ (i, j) \mid i = PZ_2, j \in CSO_2 \cup \{FD\}\},$$

$$A_7 = \{ (i, j) \mid i \in CSO_2, j \in CSO_2 \cup \{FD\}\},$$

$$B_1 = \{ (i, j) \mid i = ID, j \in \vartheta_D\}, \qquad B_2 = \{ (i, j) \mid i \in \vartheta_D, j = FD\}.$$

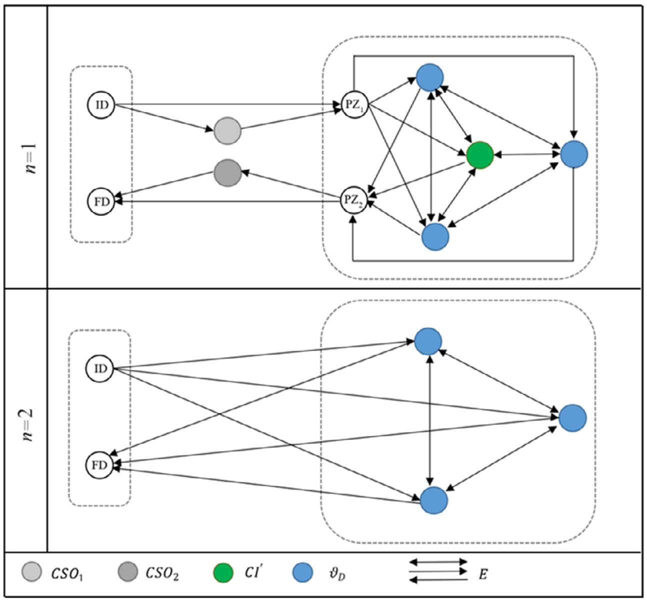

Fig. 2. The graph of the problem.

Then, $FVI_j = \{i| \, (i, j) \in E\}$ and $FVJ_i = \{j| \, (i, j) \in E\}$ represent the feasible former and latter vertices of a vertex, such that the linking arc is admissible. Figure 2 illustrates the described graph.

As the figure illustrates, our approach merges the EVRP and corridor electrification into a cohesive framework. The EVRP focuses on optimizing routes for E-AGVs within the target zone, while the corridor electrification aspect addresses the efficient routing of these vehicles over longer linking distances, considering the availability of charging infrastructure along these corridors.

The set of potential platoons, distinguished by P, is derived based on the subset of available drivers that the platform designates as platoon leaders. Each potential platoon is uniquely identified by its leading driver, and the number of potential platoons is accordingly limited by the number of available leading drivers. F represents the set of carriers. Each carrier $l \in F$ has a limited number of E-AGVs and

Trucks, represented by K_l^1 and K_l^2, respectively. Then, $K^1 = K_1^1 \cup \ldots \cup K_l^1 \cup \ldots \cup K_L^1$ and $K^2 = K_1^2 \cup \ldots \cup K_l^2 \cup \ldots \cup K_L^2$ show the union of the E-AGVs and trucks of the carriers, respectively. The decision-making process is interdependent and sequential. Initially, the platform specifies service fees, routing, and platooning decisions to minimize its total cost. Subsequently, carriers assess these decisions to determine whether to deploy their vehicles based on the proposed service fees and routes or reject the offer. This interactive decision-making process is modeled as a two-level constrained Stackelberg competition, where the platform acts as the leader and the carriers as followers. While the platform initiates the decision-making process, it ensures alignment with the carriers' incentives, creating a mutually beneficial arrangement. This approach is grounded in game theory principles, with the platform's initial decisions made in anticipation of the carriers' likely responses, thereby accommodating their decisions within its strategy. The notations used to formulate the model are presented as follows:

Sets	
$\{ID\}, \{FD\}$	Initial and final depots, respectively
CSO_1, CSO_2	Set of charging stations in the linking segment and its duplicate, respectively
$\{PZ_1\}, \{PZ_2\}$	Platooning node in the target zone and its duplicate, respectively
ϑ_D	Set of demand points
CI'	Set of dummy nodes illustrating charging stations (CI) and their copies in the target zone
FVI_j	Admissible set of former vertices of vertex j
FVJ_i	Admissible set of latter vertices of vertex i
K	Set of the vehicles of all carriers
F	Set of carriers
P	Set of potential platoons to be formed, governed by the number of available platoon drivers
Parameters	
D_i	Demand of $i \in \vartheta_D$
UB	Maximum allowed number of E-AGVs in a platoon
LB	Minimum allowed number of E-AGVs in a platoon ($LB = 2$)
T_i^n	Service time of vertex i for mode n
$T_{ij}'^n$	Travel time of arc (i,j) for mode n
TA_i	Lower bound for admissible service time at vertex i
TB_i	Upper bound for admissible service time at vertex i
Cap^{k^n}	Capacity of the vehicle k^n, $n = 1, 2$ (where k^1 represents E-AGVs, and k^2 trucks)
BA_{ls}	Binary parameters stating whether carrier l has a contract with station s ($s \in CSO_1 \cup CI$)
AV_l^n	Available vehicles of carrier l of mode n
β^{k^n}	Minimum acceptable profit rate of vehicle k^n ($n = 1, 2$)
CT^n	Unit energy consumption cost of mode n
CL^n	Driver wage for mode n ($CL^1 = 0$)
CLP^p	Wage paid by the platform to the leading driver of platoon p
CA^{k^n}	Fixed acquisition cost for vehicle k^n ($n = 1, 2$)
CE	Emission penalty cost per gram
$e_{ij}^{k^n}$	Energy consumption of vehicle k^n ($n = 1, 2$) for traveling arc (i,j)
$ce_{ij}^{k^n}$	Carbon emission of vehicle k^n for traveling arc (i,j) ($ce_{ij}^{k^1} = 0$)
Q	Maximum Battery capacity of the E-AGVs
$M_1, \ldots, M_7$	Upper bounds on the left-hand side of respective constraints, used to enable conditional logic
$m_1, \ldots, m_8$	Lower bounds on the left-hand side of respective constraints, used to enable conditional logic
Decision variables	
$x_{ij}^{k^n}$	1: if vehicle k^n travels from i to j 0: otherwise
$v_p^{k^1}$	1: if k^1 (E-AGV) joins platoon p 0: otherwise
σ_p	1: if platoon p is formed 0: otherwise
z^{k^n}	1: if vehicle k^n is used 0: otherwise
ζ_l	1: if carrier l joins the platform 0: otherwise
u_{ijp}	1: if platoon p travels from i to j 0: otherwise
$ST_i^{k^n}$	Time when vehicle k^n starts to service vertex i

Continued

AT^{k^1}	Time when vehicle k^1 (E-AGV) arrives at the platooning node (PZ_2)
TW^{k^1}	Waiting time of vehicle k^1 (E-AGV) to join its platoon at the platooning node (PZ_2)
STP_{ip}	Time when platoon p starts to service vertex i
$BL_i^{k^1}$	Battery level of vehicle k^1 (E-AGV) arriving at vertex i
W^{k^n}	Service fee announced for vehicle k^n for serving demand points
RW^{k^n}	Service fee paid to vehicle k^n for serving demand points

3.1. Optimization **model of the platform**

$$P_1 : min\ Z_1 = \sum_{n=1,2} \sum_{k^n \in K^n} RW^{k^n} + \sum_{p \in P} CLP^p \sigma_p, \tag{1}$$

s.t.

$$\sum_{n=1,2} \sum_{k^n \in K^n} y_i^{k^n} = 1 \quad \forall i \in \vartheta_D, \tag{2}$$

$$\sum_{j \in FVJ_i} x_{ij}^{k^n} = z^{k^n} \quad \forall i = ID, k^n \in K^n, n = 1, 2, \tag{3}$$

$$\sum_{i \in FVI_l} x_{il}^{k^n} - \sum_{j \in FVJ_l} x_{lj}^{k^n} = 0 \quad \forall l \in \vartheta, k^n \in K^n, n = 1, 2, \tag{4}$$

$$\sum_{i \in \vartheta_D} \sum_{j \in FVJ_i} D_i x_{ij}^{k^n} \leq Cap^{k^n} \quad \forall k^n \in K^n, n = 1, 2, \tag{5}$$

$$\sum_{j \in FVJ_i} x_{ij}^{k^1} = \sum_{p \in P} v_p^{k^1} \quad \forall i = ID, k^1 \in K^1, \tag{6}$$

$$\sum_{j \in FVJ_i} u_{ijp} \leq \sigma_p \quad \forall i = ID, p \in P \tag{7}$$

$$x_{ij}^{k^1} = \sum_{p \in P} u_{ijp} v_p^{k^1} \quad \forall i \in \{ID\} \cup CSO_1 \cup \{PZ_2\} \cup CSO_2, j \in FVJ_i, k^1 \in K^1, \tag{8}$$

$$\sum_{i \in FVI_l} u_{ilp} - \sum_{j \in FVJ_l} u_{ljp} = 0 \quad \forall l \in CSO_1 \cup CSO_2, p \in P \tag{9}$$

$$u_{ijp} = 0 \quad \forall i \in \{PZ_1\} \cup CI' \cup \vartheta_D, j \in FVJ_i, p \in P \tag{10}$$

$$\sum_{j \in FVJ_i} x_{ij}^{k^1} \leq \sum_{l \in F} BA_{ls} \zeta_l \quad \forall s \in CSO_1, i \in (CSO_1 \cup CSO_2)_s, k^1 \in K^1, \tag{11}$$

$$\sum_{j\in FVJ_i} x_{ij}^{k^1} \le \sum_{l\in F} BA_{ls}\zeta_l \quad \forall s \in CI, i \in\ CI'_s, k^1 \in K^1, \tag{12}$$

$$LB\,\sigma_p \le \sum_{k^1\in K^1} \nu_p^{k^1} \le UB\,\sigma_p \quad \forall p \in P, \tag{13}$$

$$STP_{ip} \le M_1\,\sigma_p \quad \forall i = ID, p \in P \tag{14}$$

$$ST_i^{k^1} = \sum_{p\in P} STP_{ip}\nu_p^{k^1} \quad \forall i \in \{ID\} \cup \vartheta \cup \{FD\} - \left(\vartheta_D, \cup CI'\right), k^1 \in K^1, \tag{15}$$

$$ST_j^{k^n} \ge (ST_i^{k^n} + T_i^n + T'^n_{ij})x_{ij}^{k^n} \quad \forall i = FVI_j, j \in \vartheta \cup \{FD\} - \{PZ_2\}, k^n \in K^n, n = 1, 2, \tag{16}$$

$$ST_j^{k^1} \ge (ST_i^{k^1} + T_i^1 + T'^1_{ij} + TW^{k^1})x_{ij}^{k^1} \quad \forall i = FVI_j, j \in PZ_2, k^1 \in K^1, \tag{17}$$

$$AT^{k^1} = \sum_{i\in FVI_j} (ST_i^{k^1} + T_i^1 + T'^1_{ij})x_{ij}^{k^1} \quad \forall j = PZ_2, k^1 \in K^1, \tag{18}$$

$$STP_{ip} = \max_{k^1\in K^1} \left(AT^{k^1}\nu_p^{k^1}\right) \quad \forall i = PZ_2, p \in P \tag{19}$$

$$TW^{k^1} = \sum_{p\in P} \left(STP_{ip} - AT^{k^1}\right)\nu_p^{k^1} \quad \forall i = PZ_2, k^1 \in K^1, \tag{20}$$

$$TA_j \sum_{i\in FVI_j} x_{ij}^{k^n} \le ST_j^{k^n} \le TB_j \sum_{i\in FVI_j} x_{ij}^{k^n} \quad \forall j \in \vartheta \cup \{FD\}, k^n \in K^n, n = 1, 2, \tag{21}$$

$$BL_j^{k^1} = \sum_{i\in\{PZ_1\}\cup\vartheta_D\cup\{PZ_2\}} (BL_i^{k^1} - e_{ij}^{k^1})x_{ij}^{k^1} + \sum_{i\in\{ID\}\cup CSO_1\cup CSO_2\cup CI'} \left(Q - e_{ij}^{k^1}\right)x_{ij}^{k^1} \quad \forall j \in \vartheta \cup \{FD\}, k^1 \in K^1, \tag{22}$$

$$W^{k^n} \le M_2 \sum_{i\in\vartheta_D} \sum_{j\in FVJ_i} x_{ij}^{k^n} \quad \forall\, k^n \in K^n, n = 1, 2, \tag{23}$$

$$RW^{k^n} = W^{k^n} z^{k^n} \quad \forall\, k^n \in K^n, n = 1, 2, \tag{24}$$

$$x_{ij}^{k^n}, y_i^{k^n}, \nu_p^{k^1}, \sigma_p, u_{ijp} \in \{0, 1\} \quad \forall i, j \in V, p \in P, k^n \in K^n, n = 1, 2, \tag{25}$$

$$ST_i^{k^n}, AT^{k^1}, TW^{k^1}, STP_{ip}, BL_i^{k^1}, W^{k^n}, RW^{k^n} \ge 0 \quad \forall i, j \in V, p \in P, k^n \in K^n, n = 1, 2. \tag{26}$$

The objective function (1) minimizes the platform costs, including the service fees paid to the carriers and the driver wages for each platoon leader. Constraints (2) ensure that each demand point is served by only one vehicle. Constraints (3) imply that a vehicle can leave the depot only if that vehicle is selected by its carrier. Constraints (4) are the flow conservation constraints. Constraints (5) guarantee that the capacity limit of each vehicle is respected. Constraints (6) ensure that an E-AGV can be applied (leaves the depot) only if it joins a platoon to travel the linking road. Constraints (7) imply that a platoon leaves the vehicle depot only if it is formed. Constraints (8) express that all E-AGVs joining a specific platoon move together within the linking road. Constraints (9) are platoon flow conservation constraints (analogous to classic VRP vehicle flow conservation). Constraints (10) imply that there are no in-platoon movements within the arcs of the target zone. Constraints (11) and (12) ensure that a BSS can be used only if at least one of the carriers in contract with this station is a part of the platform. Furthermore, it shows that a carrier allows battery pooling only if it is a part of the platform. $(CSO_1 \cup\ CSO_2)_s$ and CI'_s show all copies of station s within the linking area and target zone, respectively. Constraints (13) ensure that the number of vehicles of a platoon is limited by a lower and upper bound. Constraints (14) specify a platoon's start time. Constraints (15) imply that the service time of an E-AGV at a node within the linking road or the vehicle depot is equal to the service time of its platoon (all in-platoon vehicles have a similar service start time). Consistency of service time is guaranteed by constraints (16) and (17). The arrival time of each E-AGV at the platooning node on its way back to the vehicle depot is determined by constraints (18). Constraints (19) express that the service time of a platoon at the platoon pooling zone (PZ_2) is the time when all E-AGVs of that platoon arrive at that node. The waiting time of each E-AGV in the platoon pooling zone is obtained by (20). Time windows are represented by constraints (21). The remaining battery level at each vertex is calculated by constraints (22). Constraint (23) guarantees that the platform announces service fees to a vehicle only if at least one demand point is planned to be served by that vehicle. Constraints (24) determine the service fee paid to each vehicle. Finally, constraints (25) and (26) imply the type of variables.

It should be noted that the parameters M_{i} and m_{i} represent left-side upper and lower bounds, respectively, used to enforce conditional constraints involving binary decision variables. Their values are derived based on feasible ranges of the respective expressions to ensure model correctness and computational stability. Care was taken to avoid excessively large values that could lead to numerical issues, while ensuring the bounds are sufficiently tight to preserve constraint validity.

Equations (8), (15)-(-20), (22), and (24) are nonlinear and are linearized as follows:

$$x_{ij}^{k^1} \le u_{ijp} + \left(1 - \nu_p^{k^1}\right) \quad \forall i \in \{ID\} \cup CSO_1 \cup \{PZ_2\} \cup CSO_2,\ j \in FVJ_i,\ p \in \mathrm{P},\ k^1 \in K^1, \tag{27}$$

$$x_{ij}^{k^1} \ge u_{ijp} - \left(1 - \nu_p^{k^1}\right) \quad \forall i \in \{ID\} \cup CSO_1 \cup \{PZ_2\} \cup CSO_2,\ j \in FVJ_i,\ p \in \mathrm{P},\ k^1 \in K^1, \tag{28}$$

$$ST_i^{k^1} - STP_{ip} \le M_3\left(1 - \nu_p^{k^1}\right) \quad \forall i \in \{ID\} \cup \vartheta \cup \{FD\} - \left(\vartheta_D, \cup CI'\right),\ p \in \mathrm{P},\ k^1 \in K^1, \tag{29}$$

$$ST_i^{k^1} - STP_{ip} \ge m_1\left(1 - \nu_p^{k^1}\right) \quad \forall i \in \{ID\} \cup \vartheta \cup \{FD\} - \left(\vartheta_D, \cup CI'\right),\ p \in \mathrm{P},\ k^1 \in K^1, \tag{30}$$

$$STP_{ip} \le M_3 \sum_{k \in K} \nu_p^{k^1} \quad \forall i \in \{ID\} \cup \vartheta \cup \{FD\} - \left(\vartheta_D, \cup CI'\right),\ p \in \mathrm{P},\ k^1 \in K^1, \tag{31}$$

$$ST_j^{k^n} - ST_i^{k^n} - T_i^n - T_{ij}^{\prime n} \ge m_2\left(1 - x_{ij}^{k^n}\right) \quad \forall i \in \{ID\} \cup \vartheta - \{PZ_2\},\ j \in FVJ_i,\ k^n \in K^n,\ n = 1, 2, \tag{32}$$

$$ST_j^{k^1} - ST_i^{k^1} - T_i^1 - T_{ij}^{\prime 1} - TW^{k^1} \ge m_3\left(1 - x_{ij}^{k^1}\right) \quad \forall i = PZ_2,\ j \in FVJ_i,\ k^1 \in K^1, \tag{34}$$

$$AT^{k^1} - ST_i^{k^1} - T_i^1 - T_{ij}^{\prime 1} \leq M_4 \left(1 - x_{ij}^{k^1}\right) \quad \forall i \in FVI_j, j = PZ_2, k^1 \in K^1, \tag{35}$$

$$AT^{k^1} - ST_i^{k^1} - T_i^1 - T_{ij}^{\prime 1} \geq m_4 \left(1 - x_{ij}^{k^1}\right) \quad \forall i \in FVI_j, j = PZ_2, k^1 \in K^1, \tag{35}$$

$$STP_{ip} - AT^{k^1} \geq m_5 \left(1 - \nu_p^{k^1}\right) \quad \forall i = PZ_2, p \in P, , k^1 \in K^1, \tag{37}$$

$$TW^{k^1} - STP_{ip} + AT^{k^1} \leq M_5 \left(1 - \nu_p^{k^1}\right) \quad \forall i = PZ_2, p \in P, k^1 \in K^1, \tag{37}$$

$$TW^{k^1} - STP_{ip} + AT^{k^1} \geq m_6 \left(1 - \nu_p^{k^1}\right) \quad \forall i = PZ_2, p \in P, k^1 \in K^1, \tag{38}$$

$$TW^{k^1} \leq M_6 \sum_{p \in P} \nu_p^{k^1} \quad \forall k^1 \in K^1, \tag{39}$$

$$BL_j^{k^1} - BL_i^{k^1} + e_{ij}^{k1} \leq 2Q \left(1 - x_{ij}^{k^1}\right) \quad \forall i \in \{PZ_1\} \cup \vartheta_D \cup \{PZ_2\}, j \in FVJ_i, k^1 \in K^1, \tag{40}$$

$$BL_j^{k^1} - BL_i^{k^1} + e_{ij}^{k^1} \geq -Q \left(1 - x_{ij}^{k^1}\right) \quad \forall i \in \{PZ_1\} \cup \vartheta_D \cup \{PZ_2\}, j \in FVJ_i, k^1 \in K^1, \tag{41}$$

$$BL_j^{k^1} - Q + e_{ij}^{k^1} \leq Q \left(1 - x_{ij}^{k^1}\right) \quad \forall i \in \{ID\} \cup CSO_1 \cup CSO_2 \cup CI', j \in FVJ_i, k^1 \in K^1, \tag{42}$$

$$BL_j^{k^1} - Q + e_{ij}^{k^1} \geq -Q \left(1 - x_{ij}^{k^1}\right) \quad \forall i \in \{ID\} \cup CSO_1 \cup CSO_2 \cup CI', j \in FVJ_i, k^1 \in K^1, \tag{43}$$

$$RW^{k^n} - W^{k^n} \geq -M_2 \left(1 - z^{k^n}\right) \quad \forall k^n \in K^n, n = 1, 2, \tag{44}$$

where constraints (27) and (289) are linearized versions of constraints (8), and constraints (29)–(31) are of constraints (15). Constraints (16) and (17) are linearized by constraints (32) and (33), respectively. Constraints (18) are linearized by constraints (34) and (35), and constraints (19) are linearized by constraints (36). Constraints (20) are linearized through constraints (37)–(39). Constraints (40)–(43) are linearized forms of constraints (22). Finally, constraints (24) are linearized by (44).

3.2. *Optimization **model of the carriers***

For each carrier $l \in F$ we have

$$P_2: \ \max \ Z_2^l = \sum_{n=1,2} \sum_{k^n \in K_l^n} \left[W^{k^n} - \left(1 + \beta^{k^n}\right) \left(\begin{array}{c} \sum_{i \in \{ID\} \cup \vartheta} \sum_{j \in FVJ_i} CT^n e_{ij}^{k^n} x_{ij}^{k^n} \\ + CL^n \sum_{j \in FVJ_{ID}} x_{IDj}^{k^n} + CA^{k^n} \sum_{j \in FVJ_{ID}} x_{IDj}^{k^n} \\ + \sum_{i \in \{ID\} \cup \vartheta} \sum_{j \in FVJ_i} CEce_{ij}^{k^n} x_{ij}^{k^n} \end{array} \right) \right] z^{k^n}, \tag{45}$$

s.t.

$$\sum_{k^n \in K_l^n} z^{k^n} \leq AV_l^n \quad \forall\, n = 1, 2, \tag{46}$$

$$\sum_{n=1,2} \sum_{k^n \in K_l^n} z^{k^n} \leq (\sum_{n \in \{1,2\}} AV_l^n)\, \zeta_l, \tag{47}$$

$$\sum_{n=1,2} \sum_{k^n \in K_l^n} z^{k^n} \geq \; \zeta_l, \tag{48}$$

$$z^{k^n}, \zeta_l \in \{0, 1\} \quad \forall k^n \in K_l^n, n = 1, 2. \tag{49}$$

The objective function (45) maximizes the total profit of each carrier, where the revenues are the received service fees from the platform, and the costs include transportation, driver wage, acquisition, and carbon emission penalty costs. Incorporating an acceptable profit rate (β) in this structure ensures that if a vehicle is exploited, its minimum profit is met. Constraints (46) guarantee that the number of available vehicles of each mode is respected. Constraints (47) and (48) imply that a carrier joins the platform if at least one of its vehicles carries out a delivery task. Constraints (49) specify the type of the variables.

3.3. Two-level Stackelberg problem

The two-level Stackelberg problem is summarized as
P_3 : min Z_1
s.t.
Constraints (2)–(7), (9)–(14), (21), (23), (25)–(44)
$\forall\, l \in F$ max Z_2^l
s.t.
Constraints (45)–(49).

Multi-stage games are solved by backward induction. First, the follower's problem is solved to obtain its best response for the different actions of the leader. Taking this best response as the input, the procedure steps backward to determine the best response of the leader. To optimize the problem of the carriers concerning the actions of the platform and obtain their best responses, it is important to note that problem P_2 is a variant of the Knapsack problem, where the terms within brackets represent the value of each item, with item weights set to 1. There are two distinct categories of items, each constrained by a maximum total weight (denoted as AV_l^n). Then, P_2 is substituted by its optimal decision rules:

$$F^{k^n} = W^{k^n} - \left(1+\beta^{k^n}\right) \begin{pmatrix} \sum_{i \in \{ID\} \cup \vartheta} \sum_{j \in FVJ_i} CT^n e_{ij}^{k^n} x_{ij}^{k^n} \\ +CL^n \sum_{j \in FVJ_{ID}} x_{IDj}^{k^n} + CA^{k^n} \sum_{j \in FVJ_{ID}} x_{IDj}^{k^n} \\ + \sum_{i \in \{ID\} \cup \vartheta} \sum_{j \in FVJ_i} CEce_{ij}^{k^n} x_{ij}^{k^n} \end{pmatrix} \forall k^n \in K_l^n, n = 1, 2, l \in F, \tag{50}$$

$$F^{k^n} \geq m_7 \left(1 - z^{k^n}\right) \quad \forall k^n \in K_l^n, n = 1, 2, l \in F, \tag{51}$$

$$F^{k^n} - F^{l^n} \leq M_7 \left(1 - \lambda^{k^n l^n}\right) \quad \forall k^n, l^n \in K_l^n, k^n < l^n, n = 1, 2, l \in F, \tag{52}$$

$$F^{k^n} - F^{l^n} \geq m_8\, \lambda^{k^n l^n} \quad \forall k^n, l^n \in K_l^n, k^n < l^n, n = 1, 2, l \in F, \tag{53}$$

$$z^{k^n} - z^{l^n} \leq 1 - \lambda^{k^n l^n} \quad \forall k^n, l^n \in K_l^n, k^n < l^n, n = 1, 2, l \in F, \tag{54}$$

$$z^{k^n} - z^{l^n} \geq \lambda^{k^n l^n} \quad \forall k^n, l^n \in K_l^n, k^n < l^n, n = 1, 2, l \in F, \tag{55}$$

$$\sum_{k^n \in K_l^n} z^{k^n} \leq AV_l^n \quad \forall\, l \in F, n = 1, 2, \tag{56}$$

$$\sum_{n=1,2} \sum_{k^n \in K_l^n} z^{k^n} \leq \Big(\sum_{n \in \{1,2\}} AV_l^n \Big)\, \zeta_l \quad \forall\, l \in F, \tag{57}$$

$$\sum_{n=1,2} \sum_{k^n \in K_l^n} z^{k^n} \geq \zeta_l \quad \forall\, l \in F, \tag{58}$$

$$\lambda^{k^n}, z^{k^n}, \zeta_l \in \{0, 1\} \quad \forall k^n \in K_l^n, n = 1, 2, l \in F. \tag{59}$$

Equality (50) specifies the value of F^{k^n} as the obtained profit of each vehicle for each mode. Constraints (51)–(55) guarantee that the profit of the carrier is maximized. More specifically, constraint (51) ensures that if the profit of a vehicle earned by the suggested service fee is negative, the carrier will not accept it. Constraints (52)–(55) guarantee that higher profit vehicles have the selection priority. Constraint (56) ensures that the number of available vehicles of each type is respected. Constraints (57) and (58) imply that a carrier joins the platform if at least one of its vehicles carries out a delivery task. Constraint (59) specifies the type of the variables. Then, the bi-level problem (P_3) is transformed into the following single-level mixed integer linear programming:

P_4 : min Z_1

s.t.

Constraints (2)–(7), (9)–(14), (21), (23), (25)–(44), (50)–(59).

4. Solution methodology

The proposed problem builds upon the classical vehicle routing problem, which is a well-known NP-hard problem. The integration of additional features, such as time windows, electric vehicle constraints (Lera-Romero et al., 2024; Yu and Anh, 2025), and platooning coordination, introduces multiple further layers of combinatorial and temporal complexity. Consequently, the extended formulation not only retains the NP-hardness of the original VRP but also presents greater intractability due to the interdependent decision variables involved. We propose a solution approach that decomposes the problem into two nested subproblems: platooning and E-AGV (and conventional

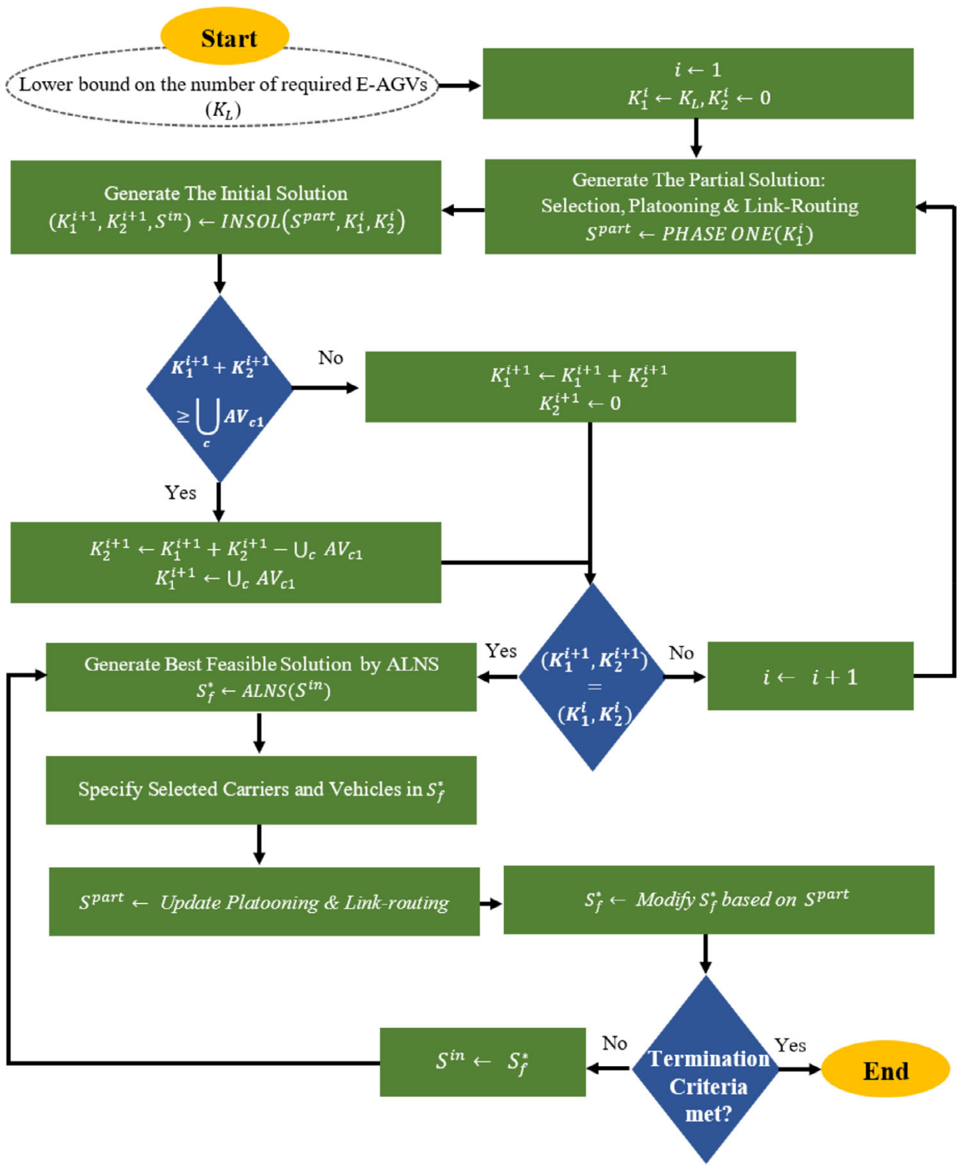

Fig. 3. Flowchart of the solution algorithm.

truck) routing. First, we create customized heuristics for the platooning problem and routing to the target zone, known as link-routing. Then, we apply a customized ALNS to determine the routing problem within the target zone. Figure 3 provides the flowchart of our proposed solution algorithm.

Our solution algorithm requires a lower bound on the number of E-AGVs as input. It then determines platooning and routing decisions to create the initial solution, which is fed into the ALNS. During ALNS iterations, vehicle choices and modes may change, necessitating updates to platooning and link-routing decisions. To determine the minimum number of E-AGVs, we create a graph where edges represent incompatibilities between demand nodes based on time windows, vehicle capacity, and battery constraints. The size of the largest clique in this graph is the lower bound on E-AGVs needed (Kontoravdis and Bard, 1995).

The vehicle wage, a component of the objective function to be minimized, is set as the carriers' minimum acceptable wage based on their costs. Thus, we can use the following cost function;

$$\Psi = \sum_{n=1,2}\sum_{k\in K}\left(1+\beta^{kn}\right)\begin{pmatrix}\sum_{i\in\{ID\}\cup\vartheta}\sum_{j\in FVJ_i} CT^n e_{ij}^{kn} x_{ij}^{kn} + CL^n \sum_{j\in FVJ_{ID}} x_{IDj}^{kn} \\ +CA^n \sum_{j\in FVJ_{ID}} x_{IDj}^{kn} + \sum_{i\in\{ID\}\cup\vartheta}\sum_{j\in FVJ_i} CEce_{ij}^{kn} x_{ij}^{kn}\end{pmatrix} + \sum_{p\in P} CL^p \sigma_p. \tag{60}$$

The components of our solution algorithm are described as follows.

4.1. PHASE ONE heuristics: selection, platooning, and link-routing

PHASE ONE heuristics determine platooning decisions and routing of platoons toward the target zone. E-AGVs are prioritized over trucks due to lower costs, no driver requirement, cheaper electricity, and zero emissions. Trucks are used only when E-AGVs are insufficient. In ALNS, we will assess the impact of replacing some E-AGVs with trucks. To determine platooning decisions, we first need to specify the E-AGVs of the carriers that will be used in our solution.

Since the linking road is significantly longer than distances within the target zone, it contributes the most to the total travel cost. Additionally, energy consumption for each carrier depends on the travel distance and vehicle characteristics. Thus, we use (ID, PZ_1) to rank carriers based on their travel costs. For each carrier, we calculate the following term as the ranking criterion:

$$EV^l =_{k\in K_l} \frac{\left(1+\beta^{k1}\right)}{PotD^k}\left(2\,CT^1 e_{ID\,PZ_1}^{k1} + CA^{k1}\right), \tag{61}$$

where $PotD^k$ is the maximum demand that an AGV of a carrier can satisfy based on its capacity. Then, carriers are selected based on their EV^l and BSS availability. Specifically, E-AGVs with the lowest EV^l are chosen if their set of contracted BSSs can ensure a feasible journey from the initial depot to the target zone. Sometimes, a carrier with a higher EV^l is chosen if its addition offers admissible travel to the target zone. After selecting carriers and vehicles, platoons are formed. We prioritize including the largest admissible E-AGVs to minimize the number of required platoons and reduce costs. Additionally, we group E-AGVs with similar electricity consumption patterns (from the same carriers) in each platoon, ensuring platoons visit BSSs when necessary for the majority of vehicles in the group.

The link-routing decisions for each platoon are determined based on the presence of E-AGVs, contracted BSSs, and existing platoons. When a platoon departs from the initial depot, it only stops at a BSS if at least one in platoon E-AGV does not have enough energy left to reach the next BSS. To decide whether the last BSS on the linking road should be visited, the energy required to travel from that BSS to PZ_1 and then to the nearest BSS in the target zone is assessed. If this exceeds the remaining battery level, the BSS is visited. Otherwise, the minimum energy required to reach a BSS on the way back to the depot is calculated, which is the energy needed to reach PZ_1 from the current node, in addition to the energy required to travel from PZ_2 to the nearest BSS in the linking road. If this exceeds the current remaining battery, at least one visit to a BSS is necessary. Since the detours to BSSs in the linking road are minimum, in that case, the last BSS should be visited.

4.2. Feasibility and penalty calculation

Our approach includes infeasible solutions in the search procedure, applying penalties for violations of vehicle capacity, battery level, and time windows. The generalized cost function of a solution S is formulated as

$$f_{gen}(S) = \Psi + \varrho_1 V_{Cap}(S) + \varrho_2 V_{BL}(S) + \varrho_3 V_{TW}(S), \tag{62}$$

where Ψ is the cost function (Equation (60)) and violations of vehicle capacity ($V_{Cap}(S)$), battery-level ($V_{BL}(S)$), and time-windows ($V_{TW}(S)$) are scaled by the penalty weights ϱ_1, ϱ_2, and ϱ_3, respectively. Every ψ_P iterations, known as the penalty update period, the penalty weights are dynamically adjusted. If a constraint has been violated in at least $\mathcal{L}^{\psi_P}$ of ψ_P iterations, its penalty weight is multiplied by ω_i; if met in at least $\mathcal{L}^{\psi_P}$ iterations, it is divided by ω_i. Penalty factors are kept within minimum and maximum limits to control the magnitude of f_{gen}.

Efficient calculation of cost function changes is crucial. The changes in capacity violations are trivially obtained in $\mathcal{O}(1)$. The changes in battery-level violations also need to be obtained. Consider an E-AGV route k in the target zone, as the sequence $\langle PZ_1, \ldots, v_i, \ldots, PZ_2 \rangle$. To calculate the battery-level violations, two variables are defined: $\Gamma^{\rightarrow}_{v_i}$, which is the energy required to travel from the last visited BSS to v_i, and $\Gamma^{\leftarrow}_{v_i}$, which is the energy required to travel from v_i to the next BSS. Then, the battery-level violations of a solution S are obtained as:

$$V_{BL}(S) = \sum_{(k,1)\in S} \sum_{v_i \in Vert(k,1)\cap(CI' \cup PZ_2)} \max\left(\Gamma^{\rightarrow}_{v_i} - Q, 0\right), \tag{63}$$

where $Vert(k, 1)$ projects visited nodes of the target zone by E-AGV k. Since we consider energy consumption independent of load, the changes in battery violations are obtained in $\mathcal{O}(1)$. We use the method from Schneider et al. (2013) to calculate time-window violations. In this approach, violations at one node do not affect subsequent nodes. Since service times at BSSs and customers are independent of the route sequence, time-window violations are calculated in $\mathcal{O}(1)$.

4.3. Initial solution

E-AGV routes require visits to BSSs, integrated into our construction and repair heuristics. When inserting a customer v at position i of a route k, we consider three additional insertions: a BSS u at position $i-1$, a BSS w at position $i+1$, or both. To select u and w from the set of contracted BSSs not yet visited and reachable with the available battery, we choose those with the lowest detours.

To construct the initial solution, we use the semiparallel construction (SPC) heuristic, proposed by Paraskevopoulos et al. (2008) for heterogeneous fleet VRP. At each iteration, an E-AGV from the available E-AGVs of each selected carrier, and a conventional truck, from the available trucks of those chosen carriers, are taken. For each vehicle, a route covering a part of the unassigned customers is constructed based on a greedy approach, while taking capacity constraints into account. For diversification, we take a restricted candidate list (RCL) of n customers with the highest evaluation score and apply roulette wheel selection to select and insert a customer. After constructing the routes, the best vehicle-route is selected, and its covered customers are removed from the set of unassigned customers. This process repeats until no further unassigned customers are left. The best vehicle route in each iteration has the lowest average cost per unit transferred (ACUT), which divides the associated costs by the sum of the demand of visited customers.

For E-AGV routes, SPC specifies the route sequence starting from PZ_1 and ending at PZ_2. The partial routes before PZ_1 and after PZ_2 are determined by link-routing and second link-routing procedures, respectively. The second link-routing procedure has the same logic as in link-routing. Considering applied E-AGVs, available BSSs, the formed platoons, and the battery level of the E-AGVs at PZ_2, each platoon leaving PZ_2 should visit a BSS only if the remaining battery level of at least one E-AGV of that platoon is not enough to reach the next charging station (or depot).

4.4. Adaptive large neighborhood search

ALNS has demonstrated strong performance in addressing routing and pickup-and-delivery problems, as evidenced by recent studies (Johannessen et al., 2024; Santos et al., 2024; Ferone et al., 2025). We adapted ALNS, proposed by Ropke and Pisinger (2006), by integrating infeasible solutions, incorporating problem-specific destroy and repair operators, local search for intensification, and introducing a BPO algorithm for selecting and placing BSSs. Algorithm 1 provides an overview of our modified ALNS approach.

4.4.1. Destroy and repair operators

Removing a customer changes the traveled distance and thereby the battery level. To address this, when removing a customer v, the algorithm checks if there exists an immediately preceding or succeeding BSS for that customer. If such stations exist, two removal scenarios are considered: removing only the customer and removing both the customer and those stations together. A destroy operator removes at least $\mathcal{G}$ nodes from the current solution, where $\mathcal{G}$ is a percentage of all nodes, randomly drawn from a given interval $[\Lambda_{min}, \Lambda_{max}]$. In addition to well-known random, worst and shawn removals, we use the following problem-specific destroy operators with a larger impact:

Station Vicinity removal (Goeke and Schneider, 2015) reorders customer visits near a BSS by selecting a random radius r, a percentage of the maximum distance between nodes in the target zone. A random BSS is chosen, and customers within a distance less than r are removed.

Route removal prioritizes truck routes over E-AGV routes, removin only after all possible truck routes have been considered. Two variants are defined: Random Route removal and Inefficient Route removal. Inefficient Route removal takes a RCL of routes with the largest ACUT and applies a roulette wheel selection to select and remove a route. If route k is the

Algorithm 1. Proposed ALNS

Input: Initial Solution (S^{in})
Output: Best obtained feasible solution (S^*_f)

$S \leftarrow S^{in}$ and $S^* \leftarrow S^{in}$
if S^{in} is feasible
  $S^*_f \leftarrow S^{in}$
end if
$i, j \leftarrow 0$
while i $< \mathbb{T}_m$ and $j < \mathbb{T}_{n-m}$
  $S' \leftarrow$ Destroy&Repair (S)
  $S' \leftarrow$ LocalSearch (S')
  $S' \leftarrow$ BPO (S')
  $S' \leftarrow$ 2$^{\text{nd}}$LinkRouting (S')
  if S' is accepted
    $S \leftarrow S'$
    if $f_{gen}(S') \leq f_{gen}(S^*)$
      $S^* \leftarrow S'$
    end if
    if S' is feasible **and** $f_{gen}(S') \leq f_{gen}(S^*_f)$
      $S^*_f \leftarrow S'$ and $j \leftarrow i$
    end if
  end if
  UpdateScore(S')
  if $0 \equiv (i+1)\ mod(\psi_P)$
  UpdatePenalty(S')
  end if
  if $0 \equiv (i-j+1)\ mod(\psi_R)$
    $S \leftarrow S^*$
  end if
  if $0 \equiv (i+1)\ mod(\psi_L)$
    AdaptSelectionScores()
  end if
  $i \leftarrow i+1$
end while
return S^*_f

only vehicle of a carrier in the current solution, its route cannot be removed due to the BSS pooling principle.

Inefficient Platoon removal tries to exclude platoons with a minimal number of E-AGVs, as their formation might not yield advantages over conventional trucks. The specific threshold for "minimal" is determined through a cost comparison between E-AGVs and trucks. Evaluating travel and emission costs based on the arc (ID, PZ1), we find that a platoon becomes viable if the number of E-AGVs exceeds:

$$\mathcal{N}^{min} = \frac{C_P}{\left(\overline{CA}^2 - \overline{CA}^1\right) + CL^2 + 2\left(CT^2 \bar{e}^2_{ID\ PZ_1} + CE^2 \overline{ce}^2_{ID\ PZ_1} - CT^1 \bar{e}^1_{ID\ PZ_1}\right)}, \tag{64}$$

where carrier-dependent cost terms are replaced with the average cost. Then, if $\mathcal{N}^{min} \geq UB$ platooning may not be beneficial at all, and there is the possibility of enhancing the solution quality by switching all vehicles to trucks. Otherwise, the platoons involving less than $\mathcal{N}^{min}$ E-AGVs are potential candidates for removal. The operator chooses the platoon with the lowest number of E-AGVs and removes all AGV routes. This removal is coupled with truck SPC-based insertion that constructs truck routes for the removed customers.

Similar to construction, each repair operator evaluates four cases (customer and preceding and/or succeeding BSSs) while adding a customer ν at a position of an E-AGV route. In addition to well-known greedy and regret insertions, we use the following problem-specific repair operators:

SPC-based insertion modifies the SPC heuristic of the construction phase by inserting customers to existing and new routes, provided that capacity constraints are met. If a new E-AGV route is to be constructed, it should either be added to an existing platoon or, if not possible, platooning and link-routing decisions need to be made.

Truck SPC-based insertion transforms the removed E-AGV routes (inefficient platoon removal) to truck routes, where the routes are constructed based on the SPC heuristic.

4.4.2. Local search

To enhance the effectiveness of the destroy and repair operators, we employ a local search (LS) method that utilizes a composite neighborhood. This includes well-known moves such as 2^*-opt (Potvin and Rousseau, 1995), Relocate (Savelsbergh, 1992), and Exchange (Savelsbergh, 1992), along with newer strategies like Resize (Hiermann et al., 2016) and StationInRe (Schneider et al., 2014). The Resize move adjusts vehicle assignments within fixed routes, ensuring vehicle modes remain unchanged, and is applied only when vehicles belong to different carriers. The StationInRe move focuses on inserting or removing BSSs from E-AGV routes.

4.4.3. BSS positioning optimization algorithm

Given the restricted ability of destroy and repair operators to position BSSs, we employ a BPO algorithm to enhance BSS selection and placement along E-AGV routes with fixed customer visits. BPO utilizes a forward labeling-based approach (Hiermann et al., 2016) to identify optimal insertion points for BSSs and selects those with minimal detours for insertion.

For each E-AGV route in the current solution, from PZ_1 to PZ_2, all BSSs within the route are eliminated, resulting in an incomplete route denoted by r'. Then, each vertex u_i ($u_i \neq PZ_2$) can be extended either by adding an immediate succeeding BSS or a null choice (no BSS is inserted). There is no need to investigate all BSSs for each vertex extension, and a subset concerning a maximal detour between u_1 and u_{i+1} is taken. A partial path from PZ_1 to a vertex $u_i \in r'$ includes the sequence of extended vertices up to that vertex. Each partial route is represented by a label $(u_i, n, R_{cost}, R_{BL}, R_{ET}, Prev)$, where n is the number of visited BSSs in the path, R_{cost} is the cost of the path, R_{BL} is the battery usage since the last visited BSS (or PZ_1), R_{ET} is the earliest start time at the current vertex, and $Prev$ is the label of extending vertex u_{i-1}. Then, if L and L' represent two labels of the paths to the same vertex u_i, L dominates L' if

$$R_{cost}(L) \leq R_{cost}(L') \text{ and } R_{BL}(L) \leq R_{BL}(L') \left(\text{if both equal to } 0: \; n(L) \leq n(L')\right) \text{ and } R_{ET}(L) \leq R_{ET}(L'). \tag{65}$$

Each label is feasible only if the battery-level constraint is met. In each route r', a BPO obtains the set of nondominated feasible labels (Ω_i) for each $i = 1, \ldots, |r'| - 1$. The final solution is obtained by taking the best label in $\Omega_{|r'|-1}$. Once a BPO improved solution is obtained, 2nd LinkRouting is applied to improve visits to BSSs of the linking road on the way back to the depot.

4.4.4. Acceptance criteria and adaptive mechanism

Our ALNS applies SA-based acceptance criteria: If a solution is improving, it is always accepted, and non-improving (deteriorating) solutions are accepted based on a probability that depends on the amount of solution deterioration and the temperature following a cooling scheme.

The destroy and repair operators are selected using a roulette wheel mechanism. The selection probability of each operator relies on its historical performance, projected by a weight. These weights are equal at the beginning of the algorithm and are updated after each ψ_L iterations, known as the adaption period (see Pourmohammad-Zia and van Koningsveld, 2024, for details).

5. Numerical experiments

This section provides the results of numerical experiments on our proposed solution. Since there are no benchmark instances for this problem, the experiments are carried out on our newly generated benchmark instances. Additionally, we tested our ALNS on EVRP benchmark instances with time windows (Schneider et al., 2014). We also conducted a case study to illustrate practical results, perform a sensitivity analysis, and derive managerial insights.

The experiments were run on a computer with an Intel® Core i7-8650U CPU, 1.9 GHz, 2.11 GHz, and 32 GB of memory available. Our developed solution algorithm, including the problem-specific heuristics together with the developed ALNS, was implemented and run on Python 3.6. We have applied IBM ILOG CPLEX Optimization Studio 12.7 as the commercial solver to obtain the optimal solutions for small-sized instances.

5.1. Parameter tuning and generation of benchmark instances

To tune the parameters of the solution algorithm, we first searched the literature for the existing values and applied values in different reasonable ranges for the new parameters. To achieve a setting with a good performance, we then investigated the impact of modifying the values of these parameters on several problem instances, each time altering one and remaining others unchanged. The selected setting provided the best results found and is represented in Table 2.

The benchmark instances comprise nine instance sets classified based on their number of customers, ranging from 5 to 150. The customer locations are randomly selected within the target

Table 2
Applied parameter setting of the developed solution algorithm

General		ALNS	
$\mathbb{T}_G$	5	$\mathbb{T}_m$	2000
$(\varrho_1,\ \varrho_2,\ \varrho_3)$	(10,10,10)	$\mathbb{T}_{n-m}$	250
$(\varrho_1^{min},\ \varrho_2^{min},\ \varrho_3^{min})$	(0.1,0.1,0.1)	ψ_R	200
$(\varrho_1^{max},\ \varrho_2^{max},\ \varrho_3^{max})$	(5000,5000,5000)	ψ_L	50
ψ_P	10	$[\Lambda_{min},\ \Lambda_{max}]$	[0.05,0.15]
$\mathcal{L}^{\psi_P}$	$0.25 \times \psi_P$	$(\varpi_1,\ \varpi_2,\ \varpi_3)$	(6,4,5)
$(\omega_1,\ \omega_2,\ \omega_3)$	(1.2,1.2,1.2)	$\mathcal{J}$	50
n	5	θ	0.6

zone, and the zone is considered to occupy an area of 0.25 km^2 for instances of 5, 10, 15, 20, and 25 customers, 0.5 km^2 for 50 customers, 0.75 km^2 for 75 customers, 1 km^2 for 100 customers, and 1.5 km^2 for 150 customers. The number of BSSs within the target zone is taken to be 10% of the number of customers ($\lceil 0.1|\vartheta_D|\rceil$), and these BSSs are randomly located within the zone.

BSSs in the linking road are located such that the distance between two successive BSSs is 20 km, with the first located at a 20-km distance from the depot. The linking road distance is 25 km for instances with 5 and 10 customers, 50 km for instances with 15 and 20 customers, 100 km for instances with 25–75 customers, and 200 km for instances with 100 and 150 customers.

In order to specify the total number of available vehicles for each mode, we first obtain an initial solution by the SPC heuristic, where the fleet contains only conventional trucks (taking both time and capacity constraints into account). This number is boosted by 30% and represents the number of available trucks and AGVs together. Then, the fleet mix is taken to involve 25%, 50%, and 75% of all available vehicles as E-AGVs. Accordingly, each set includes three groups with different numbers of available E-AGVs and trucks and each group contains two instances with different randomly generated locations. The vehicles (of each mode) within the carriers are homogenous, while they can differ in capacity, acquisition cost, and energy consumption between the carriers. The number of carriers for the first five sets is taken as three. This value is 6 for the sixth, 8 for the seventh, 10 for the eighth, and 12 for the ninth set.

The battery energy required to travel an arc is obtained as from Zhang et al. (2018). Distances are transformed into travel time by speeds of 75 km/hour for trucks and 55 km/hour for E-AGVs in the linking road and 30 km/hour for trucks and 25 km/hour for E-AGVs within the target zone. The battery capacities are taken as 120 kWh (Earl et al., 2018). The number of admissible E-AGVs of a platoon is confined between (2,5). The unit energy cost is 1.27 € for trucks and 0.27 € for E-AGVs. The carbon emission penalty is considered as 0.0003 €/g.

5.2. *Experiment on existing EVRP with time-windows benchmark instances*

We conduct experiments on existing benchmark instances for EVRP with time-windows (Schneider et al., 2014) to assess the performance of our proposed ALNS. In this regard, the automation assumption is relaxed. Therefore, all platooning and link routing-related procedures are eliminated, and the algorithm starts with the classic SPC to obtain an initial solution. In this way, our ALNS is decreased to solve a classic EVRP with time windows.

In Table 3, the performance of our ALNS in these instances is compared with those of Schneider et al. (2014), Goeke and Schneider (2015), Keskin and Çatay (2016), and Schiffer and Walther (2018). The second column of the table provides the best-known solution (BKS) by Schneider et al. (2014). The next columns present the gap of these studies to the BKS. In Goeke and Schneider (2015), Schiffer and Walter (2018), and ours, the best results of 10 runs are reported, while Keskin and Çatay (2016) provide the best result of the entire experiment. It should be noted that these algorithms were run on different platforms, so a precise comparison of time is not possible.

[a]A negative gap indicates that the solution improves upon BKS by achieving a smaller objective function value.

The average gap of the results obtained by our ALNS to BKS is 0.69% better than Schneider et al. (2014), 0.27% better than Goeke and Schneider (2015), 5% better than Schiffer and Walter (2018), and 0.39% worse than the average gap of Keskin and Çatay (2016), which was associated with the best result of the entire experimental study and not 10 runs. Our ALNS improves BKS in 19 cases and provides better results than Schneider et al. (2014), Goeke and Schneider (2015), Keskin and Çatay (2016), and Schiffer and Walter (2018) in 34, 36, 17, and 21 cases, respectively.

5.3. *Experiment on newly generated benchmark instances*

In this section, experimental results on our newly generated benchmark instances are provided. We first use the instance sets with 5–25 customers to analyze the performance of our algorithm on small-sized instances. To this end, the results of the proposed solution algorithm are compared with the optimal (global or local) solutions provided by CPLEX. Table 4 provides the results of our experiments on small-sized instances. For CPLEX, the objective function value (Z_1), number of applied E-AGVs (n_E), number of applied trucks (n_T), number of formed platoons (n_P), and run time (t) in seconds are reported. The computing time of CPLEX is limited to 2 hours (7200 seconds). So, for instances that have reached this upper bound, optimality is not guaranteed. In our proposed solution algorithm, Z_1, n_E, n_T, and n_P are associated with the best-found solution in ten runs of the algorithm. Δ_{CPLEX} represents the gap between the obtained objective function value and the one provided by CPLEX.

Our proposed algorithm performs well in solving small-sized problems to optimality quickly. For instances with 5 and 10 customers, the optimality of CPLEX results is guaranteed, as the computation time was shorter than two hours. Since the gap is zero in these instances, the results obtained by our proposed algorithm are also globally optimum. In instances with 15 customers, CPLEX was not able to reach the global optimum within two hours. However, the gap of CPLEX to the linear relaxation of the objective function found in iterations of branch and bound was less than 0.06%. This implies that the obtained solutions by CPLEX are either globally optimum or very near to the global optimum. In the larger instance set of 20 customers, CPLEX was not able to provide the optimal solution either. In these six instances, our solution algorithm obtained results equal to or smaller than those achieved by CPLEX. In addition to superior solution quality, our method demonstrates significant computational efficiency compared to CPLEX. With execution time limits of 10 seconds for instances with 10 customers, 100 seconds for 15 customers, and 200

Table 3
The results of experiments on existing benchmark instances

Instance	BKS	Δ_{BKS}[a] (%)				
		Schneider et al. (2014)	Goeke and Schneider (2015)	Keskin and Çatay (2016)	Schiffer and Walter (2018)	Our proposed ALNS
c101	1053.83	0.00	0.00	0.00	0.00	0.00
c102	1056.47	0.07	0.07	−0.03	0.82	−0.13
c103	1041.55	0.00	−0.26	−3.82	−0.18	−0.64
c104	979.51	0.13	−0.76	−2.85	−0.80	−1.45
c105	1075.37	0.00	0.00	0.00	0.00	0.00
c106	1057.65	0.02	0.00	0.00	0.00	0.00
c107	1031.56	0.00	0.00	0.00	0.00	0.00
c108	1100.32	0.00	−0.13	−7.69	−0.40	−0.42
c109	1036.64	1.47	−0.29	3.14	0.61	−0.29
c201	645.16	0.00	0.00	0.00	0.00	0.00
c202	645.16	0.00	0.00	0.00	0.00	0.00
c203	644.98	0.00	0.00	0.00	0.00	0.00
c204	636.43	0.00	0.00	0.00	0.00	0.00
c205	641.13	0.00	0.00	0.00	0.00	0.00
c206	638.17	0.00	0.00	0.00	0.00	0.00
c207	638.17	0.00	0.00	0.00	0.00	0.00
c208	638.17	0.00	0.00	0.00	0.00	0.00
r101	1663.04	0.57	0.46	0.96	0.00	0.16
r102	1488.97	3.15	0.26	2.07	−0.30	0.00
r103	1285.96	1.06	−0.31	2.06	−0.92	0.00
r104	1088.43	0.00	0.21	−1.52	1.32	0.00
r105	1461.25	0.84	−0.51	−5.34	0.96	−1.29
r106	1344.66	0.00	−1.13	−5.09	−1.40	−1.53
r107	1154.52	0.00	−0.26	−0.53	−0.53	−0.53
r108	1050.04	1.51	1.22	0.15	0.31	0.00
r109	1294.05	0.00	−2.53	−6.13	−0.57	−2.53
r110	1126.74	1.49	1.30	−2.56	1.98	−0.32
r111	1106.19	1.62	1.61	0.27	1.00	0.29
r112	1026.52	0.00	0.02	1.19	−0.96	−0.08
r201	1264.82	0.00	0.21	0.07	−0.04	0.00
r202	1052.32	0.00	0.05	0.00	0.16	0.00
r203	895.91	1.89	0.35	−0.04	0.01	−0.04
r204	788.67	0.24	−0.73	−0.98	−1.08	−0.87
r205	988.67	0.00	0.14	−0.13	−0.13	0.00
r206	922.70	0.27	0.23	0.00	−0.06	0.00
r207	848.53	0.49	0.05	−0.16	−0.63	0.00
r208	736.60	0.00	0.44	−0.07	−0.07	−0.07
r209	872.36	0.00	0.16	−0.13	−0.59	0.00
r210	847.06	0.00	0.34	−0.40	−0.18	0.00
r211	847.45	2.21	−1.41	−10.14	−2.23	−2.31
rc101	1726.91	0.24	0.47	0.24	0.11	0.00
rc102	1659.53	−6.32	−6.15	−6.50	−6.50	−6.32
rc103	1351.15	0.18	0.02	0.04	0.07	0.00

Continued

Table 3
(Continued)

Instance	BKS	Δ_{BKS}[a] (%)				
		Schneider et al. (2014)	Goeke and Schneider (2015)	Keskin and Çatay (2016)	Schiffer and Walter (2018)	Our proposed ALNS
rc104	1229.82	1.58	−0.05	0.21	0.32	0.00
rc105	1475.31	0.55	0.62	−0.14	0.24	0.00
rc106	1436.61	0.25	0.17	−1.50	−0.93	0.00
rc107	1275.89	0.00	0.04	0.56	0.09	0.04
rc108	1204.87	2.82	−0.35	0.35	−0.62	−0.42
rc201	1444.94	0.16	0.13	0.13	0.14	0.16
rc202	1412.91	0.00	0.45	2.65	−0.34	0.00
rc203	1073.98	0.40	−0.01	−0.44	−1.75	0.00
rc204	885.35	0.44	0.80	0.24	−0.09	0.00
rc205	1282.58	3.05	0.56	−0.39	−1.57	0.00
rc206	1190.75	0.03	0.06	1.42	0.01	−0.03
rc207	995.52	0.00	1.01	−0.10	−1.05	0.00
rc208	837.82	0.03	−0.18	0.42	−0.11	−0.04
Average gap (%)		0.36	−0.06	−0.72	−0.28	−0.33
Average time (minutes)		15.34	2.78	-	3.77	4.23

seconds for 20 customers, the gaps between the solutions found by CPLEX and our method range between 94–98%, 79–88%, and 81–92% for 20, respectively.

Next, we evaluate the performance of our algorithm across new benchmark instances ranging from 25 to 150 customers. We report the objective function value of the BKS achieved during algorithm testing. Additionally, we analyze the algorithm's performance with and without hybridization with LS and BPO, presenting results from 10 runs, including the objective function value (Z_1), its gap to BKS (Δ_{BKS}) number of applied E-AGVs (n_E), the number of applied trucks (n_T), the number of formed platoons (n_P), and run time (t), as shown in Table 5.

By comparing the results of the three fleet mixes in these instances, one can observe that the increase in AGVs' penetration considerably improves the costs of the system. This highlights the efficiency of our proposed E-AGV platoon setting for freight transportation. Furthermore, the results show that the hybrid solution approach outperforms ALNS, without a notable increase in execution time.

5.4. Case study

The East and Southeast logistic corridors are critical lifelines for the economic prosperity of the Netherlands. As freight transportation demands rise and traffic congestion worsens in these corridors, expanding their capacity and optimizing traffic flow becomes essential. Connected corridors are rigorous solutions for this challenge. Extending high-level automated driving and platooning to these corridors is one of the main actions for technological developments toward connected corridors (Top Corridors Program, 2018).

Table 4
The results of experiments on newly generated small-sized benchmark instances

Instance	CPLEX					Proposed solution algorithm					
	Z_1	n_E	n_T	n_P	t (seconds)	Z_1	Δ_{CPLEX} (%)	n_E	n_T	n_P	t (seconds)
SI-5-1-25%	269.017	3	0	1	3.79	269.017	0.00	3	0	1	3.32
SI-5-1-50%	269.017	3	0	1	3.26	269.017	0.00	3	0	1	3.21
SI-5-1-75%	269.017	3	0	1	3.44	269.017	0.00	3	0	1	3.29
SI-5-2-25%	269.061	3	0	1	4.31	269.061	0.00	3	0	1	3.64
SI-5-2-50%	269.061	3	0	1	4.61	269.061	0.00	3	0	1	3.71
SI-5-2-75%	269.061	3	0	1	4.17	269.061	0.00	3	0	1	3.59
SI-10-1-25%	675.005	3	2	1	214.62	675.005	0.00	3	2	1	4.42
SI-10-1-50%	427.298	5	0	1	279.88	427.298	0.00	5	0	1	6.19
SI-10-1-75%	427.298	5	0	1	281.45	427.298	0.00	5	0	1	6.23
SI-10-2-25%	675.146	3	2	1	276.83	675.146	0.00	3	2	1	4.88
SI-10-2-50%	427.389	5	0	1	337.61	427.389	0.00	5	0	1	6.45
SI-10-2-75%	427.389	5	0	1	331.06	427.389	0.00	5	0	1	6.73
SI-15-1-25%	1261.602	3	4	1	7200	1261.593	−0.0008	3	4	1	59.31
SI-15-1-50%	891.856	6	1	2	7200	891.856	0.00	6	1	2	72.16
SI-15-1-75%	744.851	7	0	2	7200	744.849	−0.0003	7	0	2	76.03
SI-15-2-25%	1261.467	3	4	1	7200	1261.467	0.00	3	4	1	58.14
SI-15-2-50%	891.789	6	1	2	7200	891.789	0.00	6	1	2	69.55
SI-15-2-75%	744.845	7	0	2	7200	744.845	0.00	7	0	2	75.81
SI-20-1-25%	1590.981	6	4	2	7200	1590.556	−0.027	6	4	2	151.39
SI-20-1-50%	1161.172	9	1	2	7200	1161.027	−0.012	9	1	2	168.41
SI-20-1-75%	1014.374	10	0	2	7200	1014.152	−0.022	10	0	2	169.08
SI-20-2-25%	1591.704	6	4	2	7200	1590.836	−0.053	6	4	2	155.48
SI-20-2-50%	1161.462	9	1	2	7200	1161.217	−0.021	9	1	2	169.13
SI-20-2-75%	1014.600	10	0	2	7200	1014.431	−0.017	10	0	2	172.17
Avg.					3672.71		−0.0064				60.51

The Rotterdam-Venlo corridor is one of the mentioned logistics corridors, which is highly important for the Netherlands since it has transformed Venlo into an international hub connecting with the German hinterland. Our case study outlines less-than-truckload freight delivery through this corridor. APM terminals Maasvlakte II (the western part of the seaport) is taken as the origin, and a districted area in the Northwest of Venlo is regarded as our target zone, depicted in Fig. 4.

The distance between Maasvlakte II and this area is 198 km. The area involves various industrial and almost no residential units. In addition to this, the features of its linking roads in terms of accessibility and its infrastructural settings have made the area a potential candidate for future automated driving purposes. The platoon pooling point is located in the western part of the target zone, intersecting the A67 highway and the area's borders for optimal accessibility. Twenty-three companies within the area that regularly receive a considerable input flow from the port are taken as our demand points. For servicing E-AGVs, there are three battery swap stations within the target zone and an additional five along the corridor. Each of the three carriers assigned to serve these demand points operates a fleet comprising a mix of E-AGVs and conventional trucks, with E-AGVs

Table 5
The results of experiments on newly generated medium and large-size benchmark instances

Instance	BKS	ALNS + LS + BPO						ALNS					
		Z_1	Δ_{BKS} (%)	n_E	n_T	n_P	t (minutes)	Z_1	Δ_{BKS} (%)	n_E	n_T	n_P	t (minutes)
MI-25-1-25%	2654.155	2654.385	0.008	6	6	2	3.64	2654.858	0.0265	6	6	2	2.87
MI-25-1-50%	2105.374	2105.488	0.005	9	3	2	4.07	2105.754	0.0180	9	3	2	3.17
MI-25-1-75%	1783.634	1783.634	0.00	12	0	3	4.09	1784.100	0.0261	12	0	3	3.21
MI-25-2-25%	2654.556	2654.556	0.00	6	6	2	3.76	2654.953	0.0150	6	6	2	2.94
MI-25-2-50%	2105.799	2105.799	0.00	9	3	2	4.09	2106.338	0.0256	9	3	2	3.19
MI-25-2-75%	1783.759	1783.759	0.00	12	0	3	4.16	1785.089	0.0746	12	0	3	3.25
MI-50-1-25%	4861.661	4861.661	0.00	12	12	3	5.09	4882.469	0.428	12	12	3	4.21
MI-50-1-50%	4074.476	4075.069	0.014	18	6	4	5.98	4321.281	6.057	18	7	4	4.75
MI-50-1-75%	3294.302	3294.572	0.008	24	0	5	6.12	3317.823	0.714	24	0	5	4.87
MI-50-2-25%	4857.321	4857.612	0.006	12	12	3	5.13	4884.959	0.569	12	12	3	4.19
MI-50-2-50%	4070.596	4070.596	0.00	18	6	4	6.04	4099.660	0.714	18	6	4	4.48
MI-50-2-75%	3290.885	3291.247	0.011	24	0	5	6.35	3461.452	5.183	24	1	5	4.99
MI-75-1-25%	7517.682	7517.682	0.00	16	20	4	6.74	7529.618	0.158	16	20	4	5.19
MI-75-1-50%	6340.674	6341.132	0.007	24	12	5	7.25	6598.647	4.068	24	13	5	5.73
MI-75-1-75%	5028.174	5028.174	0.00	36	0	8	7.97	5098.832	1.405	37	0	8	6.38
MI-75-2-25%	7515.005	7515.005	0.00	16	20	4	6.53	7548.206	0.442	16	20	4	5.23
MI-75-2-50%	6337.548	6337.738	0.003	24	12	5	7.24	6594.127	4.048	24	13	5	5.72
MI-75-2-75%	5020.504	5021.609	0.022	36	0	8	7.81	5094.013	1.464	37	0	8	5.94
LI-100-1-25%	17238.127	17335.639	0.565	20	28	4	8.74	17827.727	3.421	20	29	4	7.54
LI-100-1-50%	14484.479	14500.141	0.108	30	18	6	9.13	14993.203	3.512	30	19	6	7.91
LI-100-1-75%	9670.312	9695.842	0.264	48	0	10	9.96	9991.366	3.321	50	0	10	8.17
LI-100-2-25%	17226.054	17283.761	0.335	20	28	4	8.55	17709.417	2.806	20	29	4	7.66
LI-100-2-50%	14478.135	14485.953	0.054	30	18	6	8.91	14982.109	3.481	30	19	6	7.81
LI-100-2-75%	9661.249	9664.823	0.037	48	0	10	9.95	10050.404	4.028	50	0	10	8.23
LI-150-1-25%	25671.059	25678.231	0.028	24	48	5	12.06	26580.947	3.544	24	50	5	10.12
LI-150-1-50%	20121.381	20124.742	0.016	48	24	10	13.11	20573.913	2.249	48	26	10	11.05
LI-150-1-75%	14702.735	14743.756	0.279	72	0	15	13.94	15554.641	5.794	72	2	15	11.67
LI-150-2-25%	25660.711	25664.046	0.013	24	48	5	11.98	26680.467	3.974	24	50	5	10.29
LI-150-2-50%	20110.449	20119.901	0.047	48	24	10	13.04	20719.393	3.028	48	26	10	11.16
LI-150-2-75%	14690.725	14712.641	0.149	72	0	15	14.18	15396.320	4.803	72	2	15	11.83
Average			0.066				7.85		2.313				6.45

constituting 50% of each fleet. Other input parameters for the problem remain consistent with our benchmark instances.

This corridor serves as a representative real-world setting for the modeled problem due to its long-haul nature, industrial concentration, and relative readiness for advanced freight technologies. It embodies the key structural and operational features targeted in our study: high freight density, existing logistics infrastructure, and national-level interest in deploying connected and automated transport systems. As such, the corridor not only validates the practical relevance of our modeling assumptions but also reflects conditions found in other high-volume freight corridors across Europe and globally, making our findings more broadly applicable.

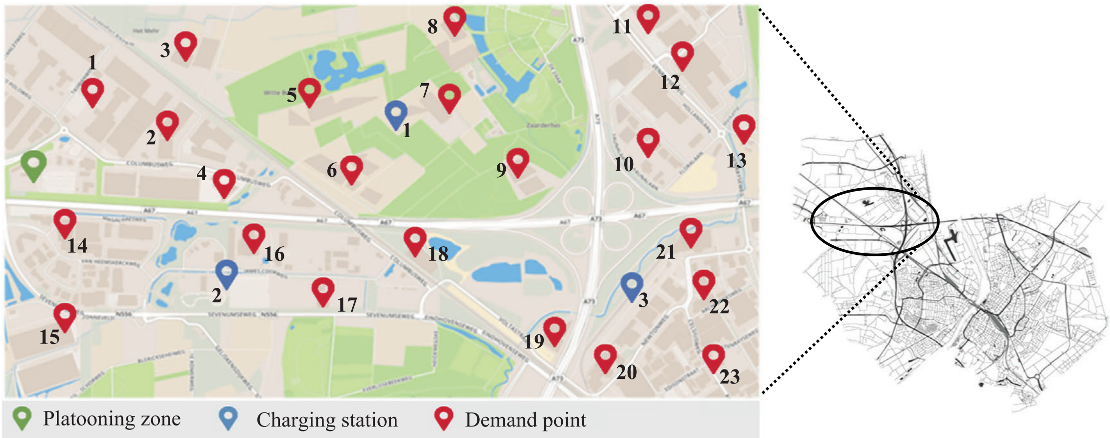

Fig. 4. Graphic illustration of our target zone.

5.4.1. Results

The results of solving the outlined use case are illustrated in Fig. 4. It is important to note that the distances in the linking route and within the target zone are depicted on different scales.

In Fig. 5, seven vehicles are used to serve demand points: five E-AGVs and two conventional trucks. The fleet mix includes two E-AGVs from carrier 1, two trucks and one E-AGV from carrier 2, and two E-AGVs from carrier 3. These five E-AGVs operate in a single platoon on the linking road, adhering to the maximum allowable AGVs per platoon. On the route from the origin to the target zone, the platoon stops at a BSS located 110 km from the origin. On the return journey from the target zone, it stops at two BSSs situated 70 and 150 km from the origin. Carrier 1's E-AGVs do not visit any BSSs within the target zone, whereas those of carriers 2 and 3 must visit one BSS to continue their trip.

5.4.2. Sensitivity analysis

The total cost of the platform is 1940.4 that involves 240 € platoon formation cost, 168.37 and 169.07 € service fees of carrier 1's E-AGVs, 408.08, 410.78, and 186.44 € service fees of the two trucks and one E-AGV of carrier 2, and finally 178.47 and 179.22 € service fees of carrier 3's E-AGVs. This suggests that E-AGVs are a cheaper transportation mode in general. Figure 6 depicts the impact of different available fleet mixes on the platform's cost and total emissions.

Figure 6 shows that by increasing the portion of applied E-AGVs in the fleet mix, the costs and emissions decrease. This introduces E-AGV platoons as a cost-efficient and environmentally friendly transportation mode. The reduction in cost and emission is considerable, up to 75%; from this point, all applied vehicles are E-AGVs, which is why the total emission has reached zero. The platform still experiences a slight decrease in costs from 75% to 100%. This reduction is not caused by the mode change but by switching to a cheaper carrier as its available E-AGVs increase.

Applying E-AGVs may not always be a more economical option compared to conventional trucks. Several factors can influence E-AGVs' competency, among which maximum admissible platoon length, energy consumption costs, the platoon formation cost, E-AGVs' acquisition costs, and

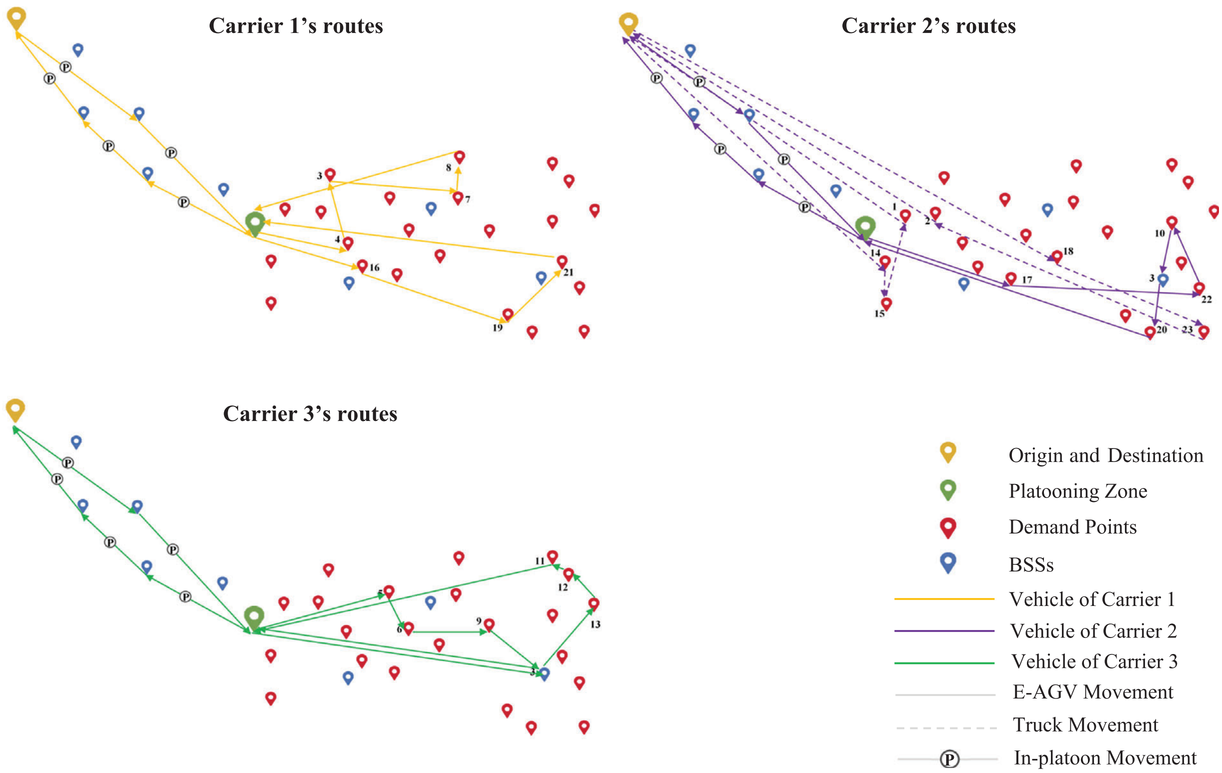

Fig. 5. Graphic representation of the results.

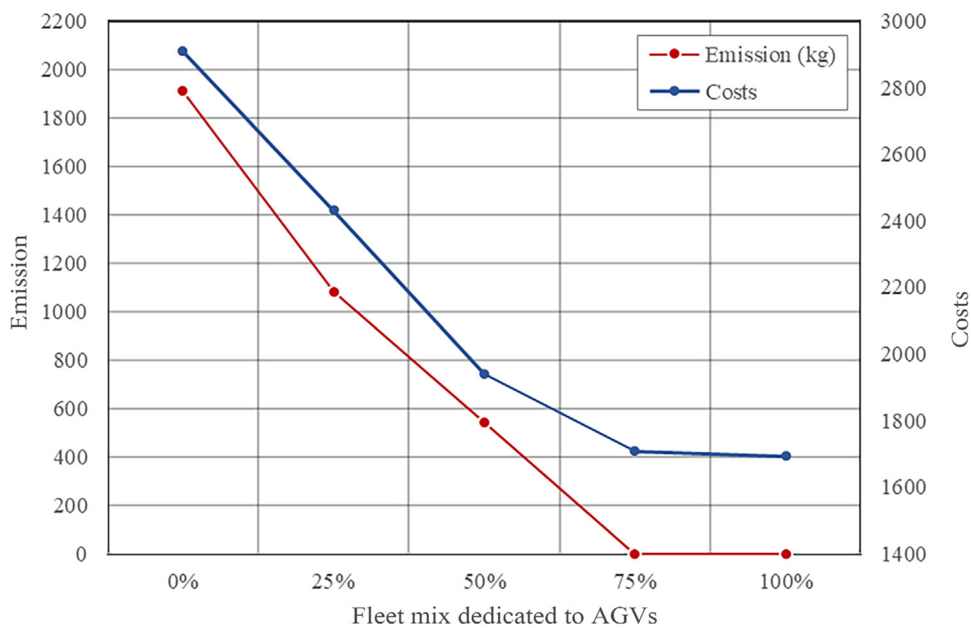

Fig. 6. The impact of E-AGVs' availability on cost and emissions.

Table 6
The impact of changes on maximum admissible E-AGVs in a platoon

UB	Total cost	n_E	n_T	n_P
2	2196.72	6	1	3
3	1962.59	6	1	2
4	1962.59	6	1	2
5	1940.41	5	2	1
6	1720.47	6	1	1
7	1503.12	6	1	1
8	1503.12	6	1	1

the availability of charging infrastructure are expected to play a notable role. In order to investigate their impact, sensitivity analyses are carried out on these parameters in the following figure and tables. More specifically, Table 6 illustrates the impact of changes on maximum admissible E-AGVs in a platoon.

The results provided in Table 6 show that increasing the admissible length of a platoon usually brings considerable cost savings to the system. This is because greater values of UB imply that fewer platoons are required to be formed, decreasing the total platoon formation costs. The number of applied E-AGVs depends on the required fleet size, the availability of the fleet mix for each carrier, and their vehicles' capacities, as well as the maximum platoon length. That is why we do not necessarily observe an increase in the number of applied E-AGVs due to the decrease in UB. For instance, for $UB = 4$, where seven vehicles are required to serve the demand points, two options can be taken: forming two platoons, one with four and the other with two E-AGVs (maximum number of available E-AGVs is six) and applying one truck or creating one platoon and using three trucks. Here, the first option results in lower costs. However, when $UB = 5$, forming the second platoon with two E-AGVs is not more cost-efficient, so two trucks are applied instead. The role of UB is better perceived when the number of required vehicles increases.

Figure 7 illustrates the impact of UB on costs and number of applied E-AGVs in our case study when customers' demanded items are settled, such that the required fleet is larger and the available vehicles of each mode are large enough so that this factor has no limiting effect in our investigation.

As Fig. 7 depicts, changes in UB lead to variations in the fleet mix from 67% to 100% dedicated to E-AGVs. Here, increasing UB, decreases the number of the formed platoon from four ($UB = 2$) to one ($UB = 10$).

Table 7 illustrates how changes in different cost parameters impact the total costs, the incorporated fleet mix, and the number of formed platoons.

The sensitivity analysis on the platoon formation cost (Table 7) indicates that reducing this parameter can lead to system-wide cost savings of up to 17%. Across different values of CL^P, the fleet composition remains predominantly comprised of E-AGVs, highlighting their cost-effectiveness even under higher platooning costs. Similar trends are observed for variations in E-AGV acquisition and energy consumption costs. Specifically, despite increases in these cost components, E-AGVs continue to dominate most routes, reinforcing their role as an economically viable mode of transportation when operating in platoons. Among the three cost elements, energy consumption has a slightly greater influence on total cost than acquisition and platooning costs.

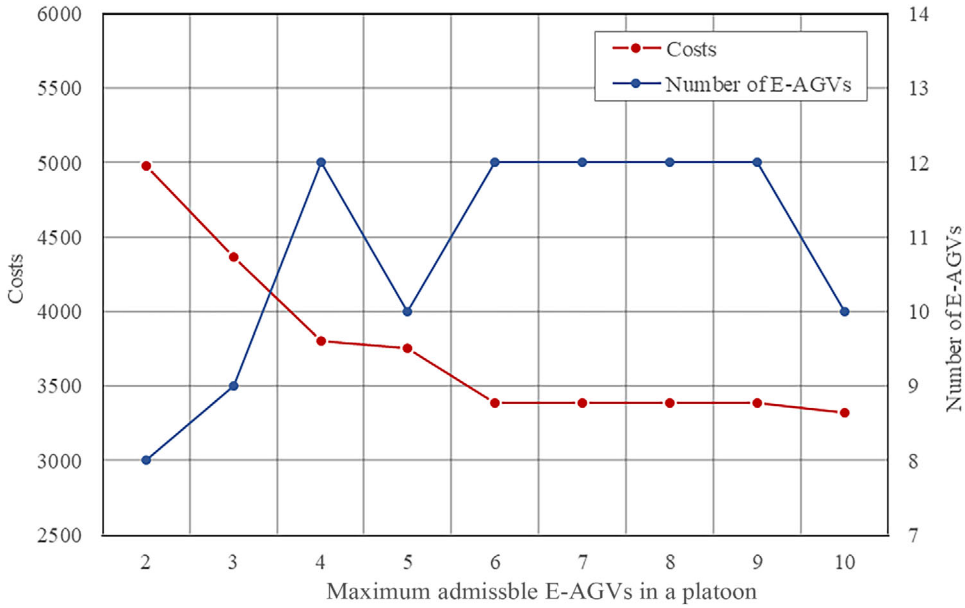

Fig. 7. The impact of UB on costs and the number of applied E-AGVs.

Table 7
The impact of changes on platoon formation and E-AGV acquisition costs

Parameter	Changes (%)	Total cost	n_E	n_T	n_P
CL^p	−75	1600.31	6	1	2
	−50	1733.54	6	1	2
	−25	1846.72	6	1	2
	0	1940.41	5	2	1
	+25	2011.52	5	2	1
	+50	2068.66	5	2	1
	+75	2127.51	5	2	1
CA^{k1}	−75	1633.02	6	1	2
	−50	1756.08	6	1	2
	−25	1859.42	6	1	2
	0	1940.41	5	2	1
	+25	2036.21	5	2	1
	+50	2123.31	5	2	1
	+75	2215.51	5	2	1
CT^1	−75	1538.91	6	1	2
	−50	1672.74	6	1	2
	−25	1826.59	6	1	2
	0	1940.41	5	2	1
	+25	2074.27	5	2	1
	+50	2208.11	5	2	1
	+75	2341.95	5	2	1

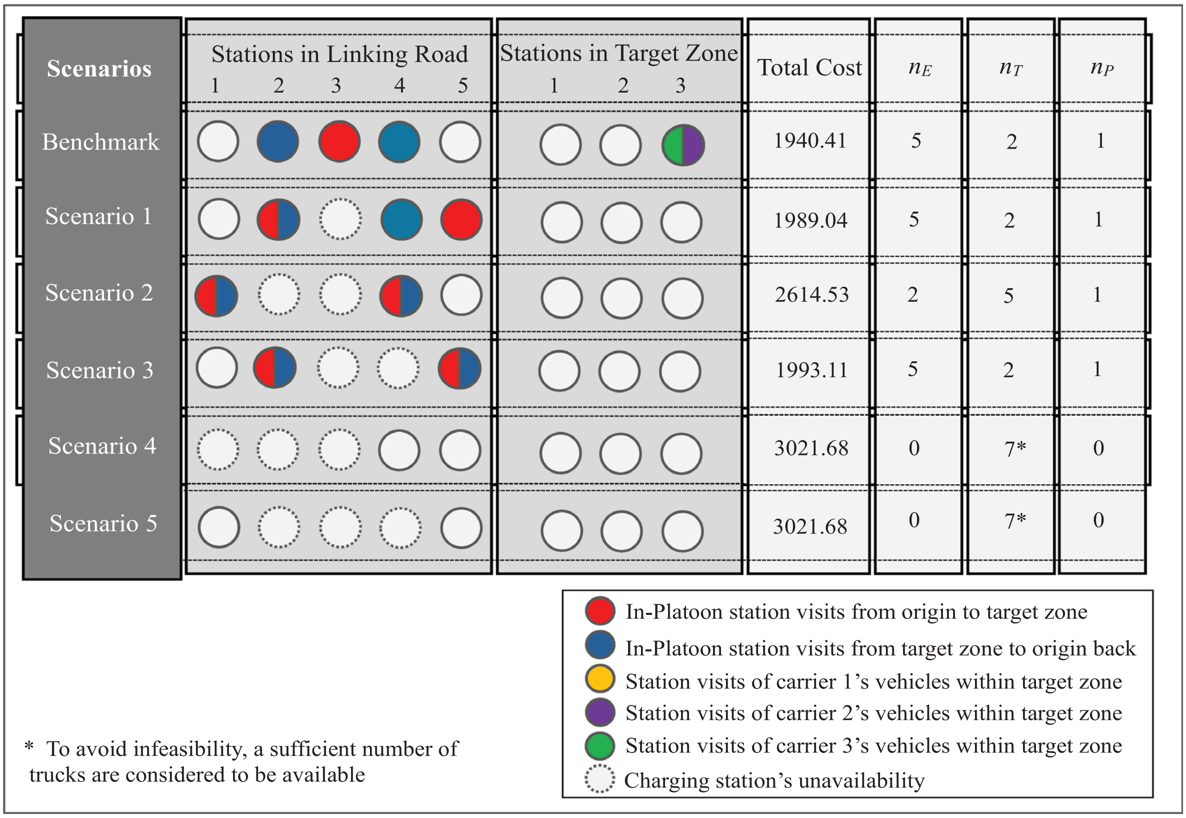

Fig. 8. Optimal solutions under different charging station availability scenarios.

As previously mentioned, another critical factor in platooning is the availability of charging stations, particularly within the designated linking road segment. Figure 8 demonstrates how variations in station availability affect the total system costs and the composition of the optimal fleet mix. It is important to note that this analysis focuses exclusively on a set of availability scenarios that significantly influence the optimal solution, as established in the benchmark results. Scenarios with negligible or no impact are excluded.

As illustrated in Fig. 8, the unavailability of certain charging stations, such as in Scenarios 1 and 3, leads to increased costs due to the need to visit alternative stations. However, it does not alter the composition of the fleet. In contrast, some scenarios make it impossible to complete the journey using the same fleet configuration as in the benchmark. For instance, in Scenario 2, only the E-AGVs operated by the first carrier are able to complete the trip within their energy limits. In Scenarios 4 and 5, the current charging infrastructure cannot meet the energy demands of the E-AGVs at all. Several other scenarios, including the unavailability of stations 1, 2, 4, or 5 individually, or even combinations such as the simultaneous unavailability of stations 1 and 2, were also examined. These cases were found to have little or no effect on costs or fleet composition. However, in the scenarios presented in the figure, total system costs can increase between 2.5% and 55%. This highlights the need to design a charging network that is resilient to disruptions affecting the availability of charging stations.

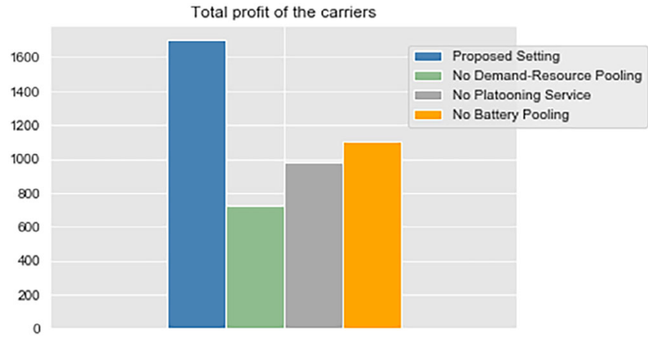

Fig. 9. The impact platform's services on carriers' total profit.

Our proposed platform-based setting provides three primary services, including demand and resource pooling, which is the main feature of collaborative transportation schemes and reduces empty runs by bundling; platooning service that facilitates applying autonomous vehicles; finally, battery pooling service that enables the carriers to visit other carriers' contracted BSSs and thereby smooths the way to use electric vehicles. Figure 9 illustrates how each of these services influences the total profit received by the carriers.

Figure 9 sheds light on the efficiency of our platform-based collaborative transportation scheme. No demand and resource pooling case depicts noncollaborative transportation and results in 57% lower profit compared to its collaborative version. This suggests that our platform-based setting not only satisfies the individual rationality of the carriers but also brings a considerable profit boost for them. We observe 42% and 35% drop in carriers' profits in no platooning and no battery pooling services, respectively. This highlights the critical role of the platform in facilitating the application of autonomy and green transportation in freight transport.

5.5. Policy implications and managerial insights

The conducted experiments provide us with valuable insights into the features of E-AGV platoons as a transfer mode that can certainly come in handy for future management of E-AGVs in the freight transport sector.

- *Clear incentives to invest in automated and electrified vehicles*: The application of E-AGV platoons provides a more cost-efficient and sustainable connection between distinct autonomous areas. More precisely, by switching from a fleet of trucks to a fleet of E-AGVs, we experienced around 42% decrease in costs and a 100% decrease in carbon emissions. This suggests that there will be enough incentives to apply autonomous electric vehicles in the near future.
- *A tipping point of adopting E-AGVs in transport corridors*: Our observations imply that the maximum admissible number of E-AGVs in a platoon has a major role in the platooning decisions and benefits. This emphasizes the impact of platooning regulations, as a first step, on the widespread application of automated driving in open areas.

- *Market price development and subsidies to accelerate adoption*: The results show that if platoon formation and E-AGV acquisition costs are managed, the cost benefits of applying E-AGVs get even higher. This suggests that, as platooning gets cheaper due to technological developments and widespread production of E-AGVs in the future, one can expect their growing application in freight transportation.
- *Collaboration for a win-win-win*: The results indicate that the carriers benefit from the proposed platform-based collaborative scheme compared to the individual setting, a classic win-win, which also allows gains for the platform. This depicts the efficiency of our collaboration mechanism and demonstrates that the proposed approach accesses a new solution space for more efficient and sustainable transportation.
- *The platform as the enabler*: We observe that the platooning and battery-pooling services are rigorously structured and provide beneficial outcomes. This highlights the critical role of the platform in facilitating the application of autonomy and electrified transportation in freight transport.

Alongside all the benefits outlined above, two important considerations should not be neglected to ensure the successful and inclusive adoption of E-AGV platooning:

- *Economic challenges for smaller carriers*: While the adoption of E-AGVs and platooning platforms promises significant cost savings and environmental benefits, smaller carriers may face economic challenges during the transition phase. High upfront investments for E-AGVs, technological upgrades, and integration into collaborative platforms could be financially burdensome for companies with limited capital. Moreover, smaller carriers might struggle with fleet renewal cycles, making it harder to align quickly with evolving standards. To address these challenges, targeted financial support mechanisms, such as subsidies for vehicle acquisition, grants for technology adoption, and preferential platform access fees, could play a crucial role. Additionally, collaborative models that allow asset sharing and flexible participation could help smaller carriers gradually adopt new technologies without disproportionate financial risks.
- *Regulatory and operational barriers*: The widespread deployment of E-AGV platoons along critical corridors is closely tied to regulatory and operational enablers. Key regulatory barriers include limitations on maximum platoon lengths, certification requirements for autonomous driving systems, and the need for standardized communication protocols across carriers and vehicle types. Operationally, the availability and interoperability of charging infrastructure remain major concerns, particularly in less urbanized areas. To overcome these barriers, coordinated actions are needed: regulatory bodies should establish clear guidelines and harmonized standards for platooning and electric vehicle operations, while industry stakeholders and policymakers must collaborate to ensure resilient, scalable charging networks. Pilot projects along priority logistics corridors could serve as testbeds for regulatory adaptation and operational fine-tuning before broader rollouts.

Finally, it is important to emphasize that these policy insights are derived from a structured corridor use case with concentrated demand, available infrastructure, and a collaborative platform with delegated authority. While the results point to strong incentives for E-AGV adoption and pooling in such settings, these conditions may not generalize to all logistics networks. For example, in long-haul trucking scenarios with sparse demand or decentralized control, the cost and coordination advantages observed here may not apply. The effectiveness of platform-based collaboration also depends on the willingness of carriers to share operational data and resources, and on regulatory frameworks that support such integration. As such, the insights in this section are best interpreted within the context of corridor-based logistics systems, where structured collaboration, infrastructure readiness, and aligned incentives can be realistically achieved.

6. Conclusion

On the path towards automated driving in open areas, platoons offer a promising solution for establishing efficient connections between various AGV-ready freight origins and destinations. This work evaluates the efficiency of platooning in an electric vehicle routing problem. Here, multiple transportation companies join forces on a shared platform to execute delivery tasks using their fleets of E-AGVs and conventional trucks. The platform serves not only as a demand and resource pooling mechanism but also facilitates platooning and sharing of electric infrastructure.

We develop an efficient solution algorithm, incorporating several problem-specific heuristics and an ALNS with customized destroy, repair, and intensification operators. Extensive numerical experiments demonstrate the robust performance of our algorithm, offering valuable insights for logistics managers. Our findings underscore the potential of E-AGV platoons to significantly reduce costs and emissions. Extensive numerical experiments demonstrate the good performance of our proposed solution algorithm and provide fruitful insights for the managers. Our findings indicate that E-AGV platoons offer significant potential to reduce costs and emissions.

While this study represents a significant advancement in the field, several promising avenues for future research emerge. Further exploration could extend E-AGV platooning into drayage operations, focusing on full container pick-up and delivery challenges. Additionally, investigating load-dependent energy consumption would provide a more realistic depiction of operational environments. Moreover, the potential congestion at shared BSSs and its impact on service times warrant attention. Future research could explore solutions such as capacity constraints implementation and scheduling optimization to mitigate congestion, ensuring efficient and timely service delivery.

Acknowledgments

This paper is supported by the project "Dynamic Fleet Management (P14-18 — project 3)" (project 14894) of the research program i-CAVE, partly financed by The Netherlands Organization for Scientific Research (NWO), domain Applied and Engineering Sciences (TTW). The third author thanks Fondecyt grant No. 1210735 and the program STIC-AmSud-22-STIC-09.

References

Afrasyabi, P., Mesgari, M. S., El-sayed, M., Kaveh, M., Ibrahim, A., Khodadadi, N., 2023. A crossover-based multi-objective discrete particle swarm optimization model for solving multi-modal routing problems. *Decision Analytics Journal* 9, 100356.

Al-Kanj, L., Nascimento, J., Powell, W. B., 2020. Approximate dynamic programming for planning a ride-hailing system using autonomous fleets of electric vehicles. *European Journal of Operational Research* 284, 3, 1088–1106.

Alnaggar, A., Gzara, F., Bookbinder, J. H., 2021. Crowdsourced delivery: a review of platforms and academic literature. *Omega* 98, 102139.

Atasoy, B., Schulte, F., Steenkamp, A., 2020. Platform-based collaborative routing using dynamic prices as incentives. *Transportation Research Record* 2674, 10, 670–679.

Behrend, M., Meisel, F., Fagerholt, K., Andersson, H., 2019. An exact solution method for the capacitated item-sharing and crowdshipping problem. *European Journal of Operational Research* 279, 2, 589–604.

Bhoopalam, A. K., Agatz, N., Zuidwijk, R., 2018. Planning of truck platoons: a literature review and directions for future research. *Transportation Research Part B: Methodological* 107, 212–228.

Boysen, N., Briskorn, D., Schwerdfeger, S., 2018. The identical-path truck platooning problem. *Transportation Research Part B: Methodological* 109, 26–39.

Caballero, W. N., Jaehn, F., Lunday, B. J., 2022. Transportation labor cost reduction via vehicle platooning: alternative models and solution methods. *Transportation Science* 56, 6, 1549–1572.

Caballero, W. N., Rios Insua, D., Banks, D., 2023. Decision support issues in automated driving systems. *International Transactions in Operational Research* 30(3), 1216–1244.

Calvo, J. A. L., Mathar, R., 2018. Connected vehicles coordination: A coalitional game-theory approach. Paper presented at the 2018 European Conference on Networks and Communications (EuCNC).

Connected Corridors Program. 2014. The United States' Connected Corridors Program. Available at https://connected-corridors.berkeley.edu/

Cross-border Corridors Project. 2017. European Commission's Cross-border Corridors Project. Available at https://digital-strategy.ec.europa.eu/en/policies/cross-border-corridors

Earl, T., Mathieu, L., Cornelis, S., Kenny, S., Ambel, C. C., Nix, J., 2018. Analysis of long haul battery electric trucks in the EU. Paper presented at the Commercial Vehicle Workshop, Graz.

Farahmand-Tabar, S., Afrasyabi, P., 2024. Multi-modal Routing in Urban Transportation Network Using Multi-objective Quantum Particle Swarm Optimization. In *Applied Multi-Objective Optimization*. Singapore: Springer Nature Singapore, pp. 133–154.

Ferone, D., Festa, P., Fugaro, S., Pastore, T., 2025. Hybridizing a matheuristic with ALNS for the optimal collection and delivery of medical specimens. *International Transactions in Operational Research* 32, 1, 90–116.

Goeke, D., Schneider, M., 2015. Routing a mixed fleet of electric and conventional vehicles. *European Journal of Operational Research* 245, 1, 81–99.

Hiermann, G., Puchinger, J., Ropke, S., Hartl, R. F., 2016. The electric fleet size and mix vehicle routing problem with time windows and recharging stations. *European Journal of Operational Research* 252, 3, 995–1018.

Hu, M., Zhou, Y., 2020. Price, wage, and fixed commission in on-demand matching. SSRN 2949513.

Intercor Project. 2016. United Kingdom's Intercor Project. Available at https://intercor-project.eu/wp-content/uploads/sites/15/2020/03/InterCor-BROCHURE-06022020-web.pdf.

Johannessen, P. B., Hemmati, A., Moshref-Javadi, M., 2024. Solving a pickup and delivery routing problem for fourth-party logistics providers. *International Transactions in Operational Research* 31, 4, 2272–2308.

Johansson, A., Nekouei, E., Johansson, K. H., Mårtensson, J., 2021. Strategic hub-based platoon coordination under uncertain travel times. *IEEE Transactions on Intelligent Transportation Systems* 23, 8277–8287.

Kashmiri, F. A., Lo, H. K., 2024. Routing of multi-modal autonomous vehicles for system optimal flows and average travel cost equilibrium over time. *Transportation Research Part C: Emerging Technologies* 159, 104483.

Keskin, M., Çatay, B., 2016. Partial recharge strategies for the electric vehicle routing problem with time windows. *Transportation Research Part C: Emerging Technologies* 65, 111–127.

Kontoravdis, G., Bard, J. F., 1995. A GRASP for the vehicle routing problem with time windows. *ORSA journal on Computing* 7, 1, 10–23.

Kung, L.-C., Zhong, G.-Y., 2017. The optimal pricing strategy for two-sided platform delivery in the sharing economy. *Transportation Research Part E: Logistics and Transportation Review* 101, 1–12.

Larsson, E., Sennton, G., Larson, J., 2015. The vehicle platooning problem: Computational complexity and heuristics. *Transportation Research Part C: Emerging Technologies* 60, 258–277.

Lera-Romero, G., Bront, J. J. M., Soulignac, F. J., 2024. A branch-cut-and-price algorithm for the time-dependent electric vehicle routing problem with time windows. *European Journal of Operational Research* 312, 3, 978–995.

Li, J., Zheng, Y., Dai, B., Yu, J., 2020. Implications of matching and pricing strategies for multiple-delivery-points service in a freight O2O platform. *Transportation Research Part E: Logistics and Transportation Review* 136, 101871.

Lin, X., Sun, C., Cao, B., Zhou, Y.-W., Chen, C., 2021. Should ride-sharing platforms cooperate with car-rental companies? Implications for consumer surplus and driver surplus. *Omega* 102, 102309.

Luo, F., Larson, J., 2022. A repeated route-then-schedule approach to coordinated vehicle platooning: Algorithms, valid inequalities and computation. *Operations Research* 70, 4, 2477–2495.

Ma, H., Shen, N., Zhu, J., Deng, M., 2020. A novel facility location problem for taxi hailing platforms: A two-stage neighborhood search heuristic approach. *Industrial Management Data Systems* 120, 3, 526–546.

Nourmohammadzadeh, A., Hartmann, S., 2016. The fuel-efficient platooning of heavy duty vehicles by mathematical programming and genetic algorithm. Paper presented at the International Conference on Theory and Practice of Natural Computing.

Paraskevopoulos, D. C., Repoussis, P. P., Tarantilis, C. D., Ioannou, G., Prastacos, G. P., 2008. A reactive variable neighborhood tabu search for the heterogeneous fleet vehicle routing problem with time windows. *Journal of Heuristics* 14, 5, 425–455.

Potvin, J.-Y., Rousseau, J.-M., 1995. An exchange heuristic for routing problems with time windows. *Journal of the Operational Research Society* 46, 12, 1433–1446.

Pourmohammad-Zia, N., Schulte, F., Negenborn, R. R., 2020. Platform-based platooning to connect two autonomous vehicle areas. Paper presented at the 2020 IEEE 23rd International Conference on Intelligent Transportation Systems (ITSC).

Pourmohammad-Zia, N., Schulte, F., Souravlias, D., Negenborn, R. R., 2020. Platooning of automated ground vehicles to connect port and hinterland: a multi-objective optimization approach. Paper presented at the International Conference on Computational Logistics.

Pourmohammad-Zia, N., van Koningsveld, M., 2024. Sustainable urban logistics: A case study of waterway integration in Amsterdam. *Sustainable Cities and Society* 105, 105334.

Pourmohammad-Zia, N., Schulte, F., González-Ramírez, R. G., Voß, S., Negenborn, R. R., 2023. A robust optimization approach for platooning of automated ground vehicles in port hinterland corridors. *Computers & Industrial Engineering* 177, 109046.

Ropke, S., Pisinger, D., 2006. An adaptive large neighborhood search heuristic for the pickup and delivery problem with time windows. *Transportation Science* 40, 4, 455–472.

Santos, M. J., Jorge, D., Bonomi, V., Ramos, T., Póvoa, A., 2024. Enhancing logistics through a vehicle routing problem with deliveries, pickups, and backhauls. *International Transactions in Operational Research*. https://doi.org/10.1111/itor.13577

Scherr, Y. O., Saavedra, B. A. N., Hewitt, M., Mattfeld, D. C., 2019. Service network design with mixed autonomous fleets. *Transportation Research Part E: Logistics and Transportation Review* 124, 40–55.

Schiffer, M., Walther, G., 2018. An adaptive large neighborhood search for the location-routing problem with intra-route facilities. *Transportation Science* 52, 2, 331–352.

Schneider, M., Sand, B., Stenger, A., 2013. A note on the time travel approach for handling time windows in vehicle routing problems. *Computers & Operations Research* 40, 10, 2564–2568.

Schneider, M., Stenger, A., Goeke, D., 2014. The electric vehicle-routing problem with time windows and recharging stations. *Transportation Science* 48, 4, 500–520.

Scholl, Joachim, Nils Boysen, and Armin Scholl, 2023. E-platooning: optimizing platoon formation for long-haul transportation with electric commercial vehicles. *European Journal of Operational Research* 304, 2, 525–542.

Sokolov, V., Larson, J., Munson, T., Auld, J., Karbowski, D., 2017. Maximization of platoon formation through centralized routing and departure time coordination. *Transportation Research Record* 2667, 1, 10–16.

Sun, L., Teunter, R. H., Babai, M. Z., Hua, G., 2019. Optimal pricing for ride-sourcing platforms. *European Journal of Operational Research* 278, 3, 783–795.

Tang, Z., Jiang, Y., Yang, F., 2023. Online stochastic weighted matching algorithm for real-time shared parking. *International Transactions in Operational Research* 30, 6, 3578–3596.

Top Corridors Program. 2018. The Netherlands' Top Corridors Program. Available at https://www.topcorridors.com/documenten/default.aspx

Wang, X., Huang, G. Q., 2021. When and how to share first-mile parcel collection service. *European Journal of Operational Research* 288, 1, 153–169.

Xue, Z., Lin, H., You, J., 2021. Local container drayage problem with truck platooning mode. *Transportation Research Part E: Logistics and Transportation Review* 147, 102211.

Yan, C., Zhu, H., Korolko, N., Woodard, D., 2020. Dynamic pricing and matching in ride-hailing platforms. *Naval Research Logistics (NRL)* 67, 8, 705–724.

You, J., Miao, L., Zhang, C., Xue, Z., 2020. A generic model for the local container drayage problem using the emerging truck platooning operation mode. *Transportation Research Part B: Methodological* 133, 181–209.

Yu, V. F., Anh, P. T., 2025. The electric vehicle routing problem with time windows, partial recharges, and covering locations. *International Transactions in Operational Research*. https://doi.org/10.1111/itor.70018

Zhang, M., Huang, G. Q., Xu, S. X., Zhao, Z., 2019. Optimization based transportation service trading in B2B e-commerce logistics. *Journal of Intelligent Manufacturing* 30, 7, 2603–2619.

Zhong, Z., Lee, J., Zhao, L., 2017. Multiobjective optimization framework for cooperative adaptive cruise control vehicles in the automated vehicle platooning environment. *Transportation Research Record* 2625, 1, 32–42.

Zhang, M., Pratap, S., Huang, G. Q., Zhao, Z., 2017a. Optimal collaborative transportation service trading in B2B e-commerce logistics. *International Journal of Production Research* 55, 18, 5485–5501.

Zhang, W., Jenelius, E., Ma, X., 2017b. Freight transport platoon coordination and departure time scheduling under travel time uncertainty. *Transportation Research Part E: Logistics and Transportation Review* 98, 1–23.

Zhang, S., Gajpal, Y., Appadoo, S. S., Abdulkader, M. M. S., 2018. Electric vehicle routing problem with recharging stations for minimizing energy consumption. *International journal of production economics* 203, 404–413.

Savelsbergh, M. W., 1992. The vehicle routing problem with time windows: Minimizing route duration. *ORSA journal on Computing* 4, 2, 146–154.